

Lawrence Berkeley National Laboratory

Recent Work

Title

A STUDY OF THE MECHANISM OF ELECTROREDUCTION AT THE DROPPING MERCURY ELECTRODE

Permalink

<https://escholarship.org/uc/item/23g2g8qd>

Author

Sanborn, Russell Hobart.

Publication Date

1955-12-01

UNIVERSITY OF
CALIFORNIA

*Radiation
Laboratory*

A STUDY OF THE MECHANISM
OF ELECTROREDUCTION AT THE
DROPPING MERCURY ELECTRODE

TWO-WEEK LOAN COPY

*This is a Library Circulating Copy
which may be borrowed for two weeks.
For a personal retention copy, call
Tech. Info. Division, Ext. 5545*

DISCLAIMER

This document was prepared as an account of work sponsored by the United States Government. While this document is believed to contain correct information, neither the United States Government nor any agency thereof, nor the Regents of the University of California, nor any of their employees, makes any warranty, express or implied, or assumes any legal responsibility for the accuracy, completeness, or usefulness of any information, apparatus, product, or process disclosed, or represents that its use would not infringe privately owned rights. Reference herein to any specific commercial product, process, or service by its trade name, trademark, manufacturer, or otherwise, does not necessarily constitute or imply its endorsement, recommendation, or favoring by the United States Government or any agency thereof, or the Regents of the University of California. The views and opinions of authors expressed herein do not necessarily state or reflect those of the United States Government or any agency thereof or the Regents of the University of California.

UCRL-3213
Chemistry Distribution

UNIVERSITY OF CALIFORNIA

Radiation Laboratory
Berkeley, California

Contract No. W-7405-eng-48

A STUDY OF THE MECHANISM OF ELECTROREDUCTION AT THE DROPPING MERCURY ELECTRODE

Russell Hobart Sanborn

December 1955

(Thesis)

Printed for the U.S. Atomic Energy Commission

A STUDY OF THE MECHANISM OF ELECTROREDUCTION AT THE DROPPING MERCURY ELECTRODE

TABLE OF CONTENTS

	<u>Page</u>
Abstract	3
Chapter 1. Review of Electrolytic Phenomena	4
Chapter 2. Method	9
Irreversible Electrode Processes at the DME	13
Method of Interpretation of the Experimental Data	23
Chapter 3. Experimental	30
Apparatus	30
Experimental Results and Interpretation	35
Conclusions	61
Chapter 4. The Formation of Unipositive Nickel by Electrolysis in Concentrated Salt Solutions	62
Acknowledgment	76
References	77

A STUDY OF THE MECHANISM OF ELECTROREDUCTION AT THE DROPPING MERCURY ELECTRODE

Russell Hobart Sanborn
Radiation Laboratory and
Department of Chemistry and Chemical Engineering
University of California, Berkeley, California

December 1955

ABSTRACT

The polarographic method was used to study the kinetics and mechanism of the electroreduction of nickelous, cobaltous, and ferrous ions in aqueous solution. The reduction was studied as a function of temperature in a non-complexing media, in chloride solutions, and in the presence of agar. It was concluded that all three ions are reduced through the electron-transfer mechanism. The slow step in the reduction of nickelous and cobaltous ions is probably the introduction of the first electron to form the unipositive states, whereas the slow step in the reduction of ferrous ion is the simultaneous introduction of two electrons. The results are compared with other characteristics of the three ions.

The reduction of Ni(II) at the dropping mercury electrode leads to the formation of Ni(I) where the concentration of various salts, such as sodium perchlorate, lithium perchlorate, calcium perchlorate, sodium chloride, or potassium chloride, is made sufficiently high. In general the formation of Ni(I) becomes clearly evident at salt concentrations of about one molar and becomes the principal process where the salt concentration is made two to three molar. Evidence for the formation of Ni(I) lies in a comparison of the observed diffusion currents with directly measured diffusion coefficients; the existence of an intermediate state of nickel that reacts with bromate; and a comparison of the amount of metallic nickel produced per Faraday of electricity in the concentrated solutions with that obtained in dilute salt solutions. Various experiments to characterize the plus-one state of nickel are described and some possible explanations of the phenomena are presented.

Chapter 1

REVIEW OF ELECTROLYTIC PHENOMENA

The current obtained from an electrolysis cell is a measure of the net rate of the electrode reaction. In turn, the current is determined by the applied potential to the cell and the species undergoing reaction at the electrode. An electrolysis reaction, such as $\text{Cu}^{++} + \underline{\text{Zn}} = \underline{\text{Cu}} + \text{Zn}^{++}$, can be considered as composed of the two half-cell reactions, $\text{Cu}^{++} + 2e^- = \underline{\text{Cu}}$ and $\underline{\text{Zn}} = \text{Zn}^{++} + 2e^-$. If the zinc anode is made much larger than the copper cathode, and zinc ions are in a sufficiently large concentration compared to that of the copper ions, the zinc electrode can be kept at a constant potential during electrolysis. Under these conditions the observed relation between current and potential is determined only by the phenomena occurring at the copper electrode. Returning to the general case, if the electrode reaction is reversible, that is, if the reactant and product are in rapid equilibrium with each other, then the electrode potential is determined by the surface activities of the reactant and product. These are connected by the Nernst equation

$$E = E^{\circ} - (RT/nF) \ln (\text{Ox})_s / (\text{Red})_s \quad (1)$$

for the reaction, $\text{Red} = \text{Ox} + ne^-$, where E° is the standard potential for the reaction when the reactant and product are at unit activity, $(\text{Ox})_s$ and $(\text{Red})_s$ are surface activities, n is the number of electrons involved in the reaction, R is the gas constant, T is the absolute temperature, and F is the Faraday. For spontaneous oxidation, the potential is given a positive sign, where for the reaction $\underline{\text{Ni}} = \text{Ni}^{++} + 2e^-$, $E^{\circ} = +0.25$ volt.

When the electrode reaction is irreversible, the Nernst equation no longer holds since the reactant and product are not in rapid equilibrium with each other. In this case the kinetics of the electrode reaction determine at what potentials the reaction takes place. Reduction occurs at more negative

potentials than the standard potential, and the oxidation reaction at more positive potentials. The deviation from the standard potential is called the overvoltage. The current is proportional to the surface activity of reactive material, $i = k' C_s$, where k' is a proportionality constant that includes the electrode area and a heterogeneous rate constant k_1 in cm/sec. A reduction current is given a positive sign. When the electrode reaction is irreversible, a large activation energy is involved, and the rate constant can be interpreted in terms of the absolute rate theory.¹ The reactive species and the reduction electrons can be pictured as moving along reaction coordinates on a potential energy surface until they reach a saddle, at which point reaction occurs. $Ox + Me^- = (\text{activated complex})$. M may take any integral value from zero to the total number of electrons in the electrode reaction. The heterogeneous rate constant may be related to the electrode potential by the equation

$$k_1 = k_1^0 \exp(-\alpha nFE/RT), \quad (2)$$

where k_1^0 is the rate constant at zero potential; $\exp(\dots)$ denotes an exponential to the base e ; n is the number of electrons in the rate-determining step; E is the electrode potential; and α is the fraction of the total electrical energy nFE that is effective in the activation process. In the literature it is sometimes referred to as the transfer coefficient. If no electrons are involved in the rate-determining step, then $k_1 = k_1^0 \exp(-\beta FE/RT)$. The decision as to whether the constant is αn or β is made after a particular mechanism for the reaction has been chosen. The choice of a zero of potential is discussed in a later section. The function of the electrode potential is to raise the energy level of electrons in the electrode with respect to the reactive species when electrons are involved in the activation reaction. The electrode potential may also play some part in activating the reactive species.

When no electrons are involved, as in activated adsorption, this latter function is its only role. In terms of the absolute rate theory,

$$k_1^0 = (kT/h)K \mu \exp(-\Delta F^*/RT), \quad (3)$$

where kT/h is a universal frequency, containing k , the Boltzmann constant, T , the absolute temperature, and h , Planck's constant; K is the transmission coefficient, or the fraction of activated complexes that yield the reaction product; μ is the thickness of the reaction layer at the electrode surface, needed to convert volume concentrations into concentration per unit area; and ΔF^* is the free energy of activation.

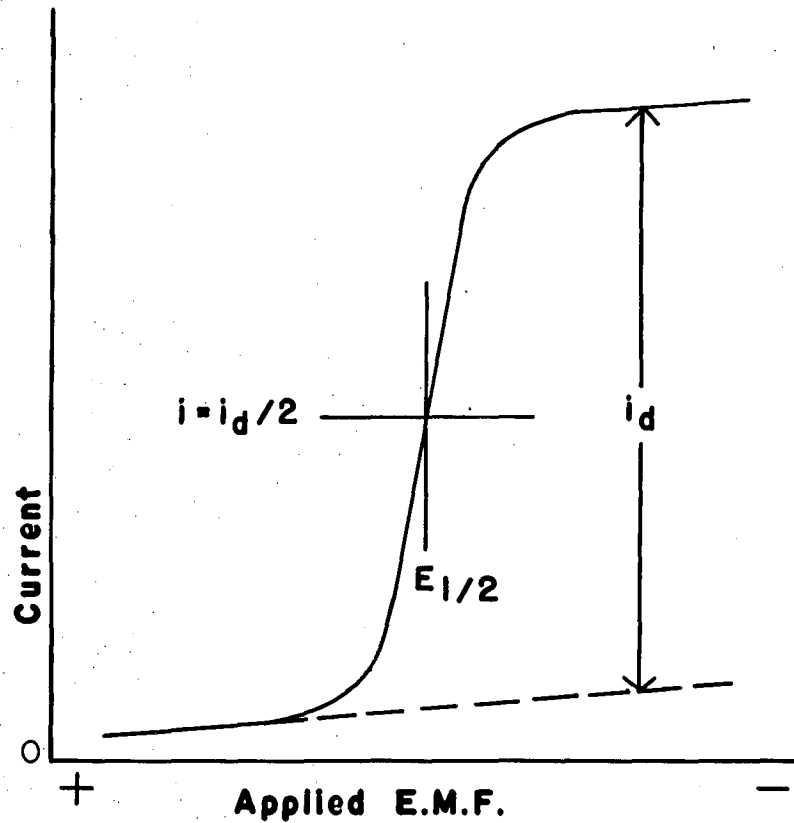
Whether or not the electrode reaction is reversible, the current obtained from the electrolysis cell is determined by the rate of chemical reaction at the electrode,

$$i = n F N/t, \quad (4)$$

where i is the current in amperes; n is the number of moles of electrons per mole of substance undergoing reaction; F is the Faraday, or 96,494 coulombs per equivalent of substance; N is the moles of substance being reacted; and t is the length of time of the electrolysis.

The electrical migration of an electro-oxidizable or -reducible species can be reduced virtually to zero by the addition of a large excess of inert electrolyte, to a concentration of 50 to 100 times that of the reactive species. The quantity of current, q , carried by any ion in the body of the solution is proportional to its concentration, c , and its velocity, u , $q = k(cu)$. The transference number of any ion is the fraction of the total current that it carries, $t_1 = q_1/\Sigma q_i$. Thus in the presence of a large excess of inert electrolyte, the transference number of the reactive species is very small, $t_1 = c_1 u_1/\Sigma c_i u_i$. In this case the reactive species, irrespective of charge, move to the electrode almost entirely by the process of diffusion.

When one of the electrodes is very small, the current is low because of the limited area of the electrode surface. If the current is plotted as a function of the applied potential, a current-voltage curve is obtained. A typical current-voltage curve obtained in polarography is presented in Fig. 1. The current is seen to be virtually zero until the decomposition potential of the reactive species is reached. What current there is at potentials below the decomposition potential is termed the residual current, and arises from the electrolysis of impurities in the solution, an almost immeasurable current from the electrolysis of the reactive species, and the energy input required by the capacity of the electrode-surface interface. After the decomposition potential, the current continually rises as the potential increases until it is limited by the rate at which reactive material can be brought to the electrode surface. In the presence of a large excess of inert electrolyte, the current is limited by the rate of diffusion of the reactive substance up to the electrode. The electrode is then said to be in an extreme state of concentration polarization, with the difference between the concentration at the surface and that in the body of the solution equal to the bulk concentration. The limiting current is then proportional to the concentration of the reactive species in the solution and is called the diffusion current, i_d . $i_d = k_s C$, where k_s is a proportionality constant dependent on the diffusion coefficient of the reactive species and the electrode geometry.



MU-10488

Fig. 1. A typical current-voltage curve.

CHAPTER 2

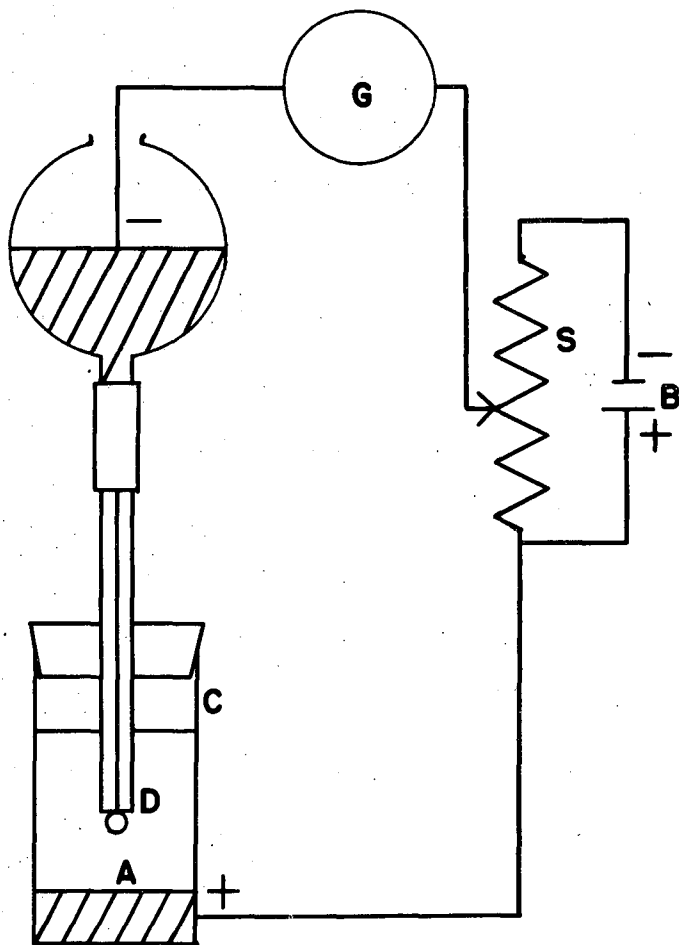
METHOD

In this research the polarographic method, utilizing the dropping mercury electrode, was used to obtain current-voltage curves. The dropping mercury electrode consists of a fine capillary of about 0.05 mm internal diameter that is connected to a mercury reservoir. Small drops form and drop off from the end of the capillary, with a drop time of from 3 to 6 seconds. Since the reactive species is usually present in small concentration in a solution containing a large excess of inert electrolyte, the currents obtained are on the order of microamperes. The second electrode most frequently used is a large pool of mercury, with some salt present in the solution that will form insoluble salts with mercury. With this set-up only the dropping electrode is polarized.

The advantages of the dropping mercury electrode are that a fresh surface of mercury is presented with every new drop, and that the current-voltage curves obtained experimentally agree satisfactorily with the theoretical equations that have been developed for the relation between current, voltage, and concentration.

The type of circuit used is described in Fig. 2. A variable potential is applied to the electrodes D and A in the electrolysis cell C by means of the slide wire S. Many instruments which utilize this simple circuit have been devised, including provision for automatically recording the current-voltage curve. These are very well described by Kolthoff and Lingane.²

The current rises from a very small value to a maximum for each drop. A galvanometer with a period greater than about fifteen seconds is chosen so that the average of the oscillation corresponds closely with the average current during the life of the drop. This average current is used in all



MU-10489

Fig. 2. A simple polarographic circuit.

equations and calculations except as otherwise stated.

Ilkovic³ and Macgillvary and Rideal⁴ derived a simple expression for the average diffusion current from Fick's laws of diffusion and the assumptions that there is no electrical migration, each drop is not influenced by its predecessor, and the drop grows spherically symmetrical about a fixed center. The Ilkovic equation at 25°C is

$$i_d = 607 n C D^{1/2} m^{2/3} t^{1/6}, \quad (5)$$

where i_d is the average diffusion current during the life of a drop in microamperes, n is the number of electrons involved in the electrode reaction, C is the concentration of the reactive material in the bulk of the solution expressed in millimoles per liter, D is the diffusion coefficient of the substance expressed in $\text{cm}^2 \text{sec}^{-1}$, m is the rate of flow of mercury from the dropping electrode in mg sec^{-1} , and t is the drop time of the electrode in seconds. This equation has been found to hold reasonably well for electrodes with approximately the same value of $m^{2/3} t^{1/6}$. The approximations introduced in the derivation, however, in effect neglect a secondary term containing the curvature of the electrode surface. Lingane and Loveridge⁵ determined a correction term for the Ilkovic equation, and the more exact expression is:

$$i_d = 607 n C D^{1/2} m^{2/3} t^{1/6} (1 + A m^{-1/3} t^{1/6} D^{1/2}), \quad (6)$$

where A was given the value of 39. From a rigorous derivation, Koutecky⁶ obtained a value of 34. The term in the parentheses is about 1.1 for most cases. For many purposes the simple Ilkovic equation is sufficient, but since the equations for the irreversible case, which is presented later, are derived with the curvature of the electrode surface taken into account, the diffusion coefficients are calculated from the more exact expression of Koutecky.

At times maxima occur in the current-voltage curves. This results from a stirring effect on the electrode surface. The stirring can be eliminated by the presence of adsorbed substances on the electrode surface, such as gelatin, agar, or organic dyes. When the presence of adsorbed substances is undesirable, a highly charged ion, such as La^{+++} , in the electrical double layer often eliminates the maximum.

Reversible electrode process. If an electrode reaction of the type



is thermodynamically reversible and very rapid compared to the rate of diffusion of the ions up to the mercury surface, then the electrode is subject to concentration polarization only. Thus the potential at each point of the polarographic wave can be expressed by means of the Nernst equation,

$$E_{\text{DME}} = E_a^\circ - \frac{RT}{nF} \ln \frac{C_a^\circ f_a}{C_s^\circ f_s}, \quad (8)$$

where C_a° is the concentration of the amalgam formed at the mercury surface, C_s° is the concentration of the ion in the layer of solution at the surface of the drop, and f_a and f_s are the corresponding activity coefficients. E_a° is the standard potential of the amalgam. Because E_{DME} , C_a° , and C_s° vary during the life of each drop, the average value in each case is used. The average surface concentration C_s° is found to be given exactly by the expression

$$\bar{i} = k_s (C_s - C_s^\circ),$$

where C_s is the concentration in the body of the solution. The proportionality constant k_s is defined by the Ilkovic equation as $607n D^{1/2} m^{2/3} t^{1/6}$ at 25°C . When the limiting diffusion current is reached, C_s°

is negligibly small compared with C_s , and $\bar{i}_d = k_s C_s$. Thus

$$C_s^0 = C_s - \bar{i}/k_s = (\bar{i}_d - \bar{i})/k_s$$

at any point along the wave. The concentration of the amalgam, C_a^0 , is proportional to the current, $C_a^0 = k' i = i/k_a$, where k_a has the same form as k_s , except that it is a function of the diffusion coefficient of the metal in the mercury. After the expressions for C_s^0 and C_a^0 have been put in the potential equation, the following relation results:

$$E_{DME} = E_a^0 - (RT/nF) \ln (f_a k_s / f_s k_a) + (RT/nF) \ln (i_d - i)/i. \quad (9)$$

The half-wave potential, $E_{1/2}$, is defined as the potential at which $i = i_d/2$, and the above equation can be simplified to

$$E_{DME} = E_{1/2} + (RT/nF) \ln (i_d - i)/i, \quad (10)$$

$$E_{1/2} = E_a^0 - (RT/nF) \ln (f_a k_s / f_s k_a). \quad (11)$$

A plot of the potential, E_{DME} , versus $\log (i_d - i)/i$ results in a straight line with a slope of $2.303 RT/nF$. Also, $E_{1/2}$ is seen to be independent of concentration of reducible material if the assumption that $\ln(f_a/f_s)$ is constant holds. This assumption is good if the concentration of the reducible species is small.

Irreversible electrode processes at the DME. The most exact expression for a kinetically controlled electrode reaction occurring at the dropping mercury electrode was derived by Koutecky,⁷ in which the expansion of the drop and the curvature of the electrode surface are taken into account. The slow reaction at the expanding drop of the dropping mercury electrode is $A + ye^- = B$. The change of concentrations of the reactant A and product B as a function of time is given by the following partial differential equations:

$$\frac{\partial a}{\partial t} = D_1 \frac{\partial^2 a}{\partial x^2} + \frac{2x}{3t} \frac{\partial a}{\partial x},$$

$$\frac{\partial b}{\partial t} = D_2 \frac{\partial^2 b}{\partial x^2} + \frac{2x}{3t} \frac{\partial b}{\partial x},$$

where a and b are the concentrations of substances A and B, x is the distance from the electrode surface, D_1 and D_2 are the diffusion coefficients of the electrode reactant and product respectively, and t is the time since the beginning of the drop. The boundary conditions used for the solution of the equations are

$$t = 0, x > 0 : a = a^* ; b = b^* ;$$

$$x = 0, t > 0 : D_1 \frac{\partial a}{\partial x} \pm D_2 \frac{\partial b}{\partial x} = 0 ; - D_1 \frac{\partial a}{\partial x} = k_2 b - k_1 a ;$$

$$x \rightarrow \infty, t > 0 : a \rightarrow a^* ; x \rightarrow \pm \infty, b \rightarrow b^* .$$

If the product of the electrode reaction B is dissolved in the solution, the plus sign in the boundary conditions is used. If it is dissolved in the electrode, the minus sign is taken; a^* and b^* are the concentrations of A and B in the body of the solution (or for B in the electrode), and k_1 and k_2 are the heterogeneous rate constants for the forward and reverse electrode reactions respectively. The current obtained is related to the concentration by the expression

$$i = nFq D_1 \left(\frac{\partial c}{\partial x} \right)_{x=0},$$

where q is the electrode area. The solution of the equations is

$$\frac{\bar{i}}{\bar{i}_{\infty}} = 7/3 X^{-7/3} \int_0^{X_1} F(X) \cdot X^{4/3} \cdot dX, \quad (12)$$

where \bar{i} is the average current at any point on the rising portion of the

current-voltage curve; \bar{i}_∞ is the average current when k_1 and k_2 approach infinity (this is the diffusion-controlled current); $F(X) = \frac{i}{i_\infty}$, the ratio of the instantaneous currents;

$$X = \frac{12}{7} \left(\frac{k_1}{\sqrt{D_1}} + \frac{k_2}{\sqrt{D_2}} \right) \sqrt{t} ;$$

and

$$X_1 = \frac{12}{7} \left(\frac{k_1}{\sqrt{D_1}} + \frac{k_2}{\sqrt{D_2}} \right) \sqrt{t_1} ,$$

t_1 being the drop time of the electrode. The above equation can be represented satisfactorily on the central portion of the current-voltage curve by the expression

$$\frac{\bar{i}}{i_d} = \frac{0.87 \left(\frac{k_1}{\sqrt{D_1}} + \frac{k_2}{\sqrt{D_2}} \right) \sqrt{t_1}}{1 + 0.87 \left(\frac{k_1}{\sqrt{D_1}} + \frac{k_2}{\sqrt{D_2}} \right) \sqrt{t_1}} \quad (13)$$

When the overvoltage is greater than 0.1 volt, k_2 is negligibly small compared to k_1 . Equations for interpreting current-voltage curves are derived from this expression. Rearranging, we obtain

$$(i_d - i)/i = 1/0.87 k_1 (t/D)^{1/2}$$

and

$$\ln (i_d - i)/i = - \ln 0.87 k_1 (t/D)^{1/2} , \quad (14)$$

where i is now used for the average current and the subscripts of t and D have been omitted. When the expression for k_1 that was previously derived is introduced, the whole expression becomes

$$\ln (i_d - i)/i = - \ln 0.87 (kT/h) K \mu (t/D)^{1/2} + \Delta F^*/RT + \alpha n FE/RT. \quad (15)$$

When $i = i_d/2$, $\ln (i_d - i)/i = 0$ and $E = E_{1/2}$.

$$E_{1/2} = (RT/\alpha nF) \ln 0.87 (kT/h) K \mu (t/D)^{1/2} - \Delta H^*/\alpha nF + T\Delta S^*/\alpha nF \quad (16)$$

since $\Delta F^* = \Delta H^* - T\Delta S^*$. Again, $E_{1/2}$ is independent of concentration and is characteristic for each reducible species at a given drop time of the electrode.

For the analysis of the current-voltage curves a plot of $\log (i_d - i)/i$ vs. $-E$ gives a slope of $-\alpha nF/2.303RT$ and the value of the half-wave potential $E_{1/2}$. Assuming that the temperature dependence of the log term is small, a plot of $-\alpha nE_{1/2}$ vs. T yields a slope of

$$-\frac{R}{F} \ln 0.87 (kT/h)(t/D)^{1/2} K \mu - \frac{\Delta S^*}{F}.$$

The quantity is chosen as the variable since αn may be a function of the temperature. The slope of a $-\alpha nE_{1/2}/T$ vs. $1/T$ plot is $+\frac{\Delta H^*}{F}$. An alternate method would be to take the intercept of the $-\alpha nE_{1/2}$ vs. T plot at the absolute zero of temperature, but a rather long extrapolation is needed. A plot of $-\alpha nE_{1/2}/T$ vs. $1/T$ requires that a choice of an absolute potential be made. A knowledge of the potential between the electrode and the site of reduction is needed. Some authors take the point of the electrocapillary maximum for the particular solution being studied. The surface tension of mercury changes with applied potential, and has a maximum value at the point where the electrical charge on the mercury is at a minimum. In cases where substances are very strongly adsorbed on the mercury surface, the potentials of maximum surface tension and minimum electrical charge do not coincide, but these cases are not involved here. The maximum in the surface tension curve is called the electrocapillary maximum. In the case of an electrolyte solution, the layer of ions at the mercury electrode surface can be considered as one plate of a condenser, with the electrode itself serving as the other plate. This phenomenon is termed that of the electrical double layer. The shape of the surface tension versus

potential curve is virtually independent of the positive ions used, whereas a change in anion can produce a marked change in the curve. At potentials more positive than the maximum, anions predominate in the electrical double layer. When the potential is 0.2 volt more negative than the maximum, only cations are in the double layer. At the potential of minimum electrical charge on the mercury, the potential between the electrode and the solution can have some finite value arising from specific adsorption of anions or orientation of water molecules on the electrode surface. Grahame⁸ suggests that the point of the electrocapillary maximum in a 0.01 M NaF solution should be the best approximation of a zero potential. This is defined as the "Rational potential" and has the value of -0.48 volt versus the normal calomel electrode. To see how significant the choice of reference potential is in the final experimental values, the "rational potential" (ECM) and the normal hydrogen electrode (NHE) were both used. The NHE is commonly used as a reference point. These two points differ by about 0.2 volt. The two methods of evaluation of ΔH^* are also compared in the experimental section.

At this point some mention should be made of previous treatments of the irreversible case. In a large number of cases plots of $\log(i_d - i)/i$ vs. E result in straight lines but with smaller slopes than predicted by the equation for the reversible curve. In general, $E_{1/2}$ for a reduction process is more negative than expected. The current-voltage curves seem to be distorted by a slow electrode reaction that requires a large activation energy. Starting from the semi-empirical concepts of Volmer⁹ and Orlemann and Kolthoff,¹⁰ Lewis¹¹ developed equations that are of the same form as Eq. (15), but with the constant

0.77 instead of 0.87. About a year before the first appearance of Koutecky's derivation,¹² Delahay¹³ derived an equation for a slow electron transfer at the dropping mercury electrode. However, the starting partial differential equations were those for a plane electrode,

$$\frac{\partial a}{\partial t} = D \frac{\partial^2 a}{\partial x^2},$$

$$\frac{\partial b}{\partial t} = D \frac{\partial^2 b}{\partial x^2},$$

and the area of the electrode was later introduced in terms of the capillary constants, $q = (4\pi)^{1/3} \gamma^{2/3} m^{2/3} t^{2/3} d^{-2/3}$, where q is the area of the drop at any instant, t , and d is the density of mercury.

The Ilkovic equation for simple diffusion can be derived from the equation for the plane electrode if the resulting expression is multiplied by a factor of $(7/3)^{1/2}$. This factor expresses the fact that the expansion of the electrode counteracts the decay in the concentration gradient at the electrode surface. Delahay utilized this factor of $(7/3)^{1/2}$ to correct his equation, but its inclusion may be somewhat arbitrary for it is not known that the same factor is applicable for the rising portion of the current-voltage curve for the slow electron transfer problem.

Lewis⁸ used $(7/3)^{1/2}$ and the result was not much different from Koutecky.⁷

Delahay's equations are in the form of complicated functions, and a considerable amount of graphical interpolation is needed to use them. Since it is impossible to obtain very precise data, it is better to use the simpler equation of Koutecky, which is a very accurate approximation to the true solution. In recent papers by Evans and Hush¹⁴ and Kivalo, Oldham, and Laitinen,¹⁵ expressions identical to those of Delahay were

given. For the limiting case of a small rate constant k_1 , both treatments reduce to the equation of Lewis. The major difficulty with using these equations is that one has either to resort to graphical interpolation or else the use of subsidiary equations containing experimental quantities that are impossible to obtain with adequate precision or accuracy. The average of each galvanometer oscillation is a fairly reproducible experimental quantity, and is utilized by Koutecky's equation. Delahay averages his equation by graphical means, whereas Kivalo, Oldham, and Laitinen attempt to use the maximum of each galvanometer oscillation, which, because of ambients in the recording process, is a much less reproducible point than the average. In addition, these latter authors utilize the change in half-wave potential, $E_{1/2}$, with the drop-time of the electrode as one means of evaluating αn . Since it is difficult to obtain half-wave potentials for irreversible reductions to a precision less than about 5 millivolts, and the maximum practical change in $E_{1/2}$ with drop-time is on the order of millivolts, this procedure can lead to quite inaccurate values of αn . In addition, since the drop-time changes with applied potential, it is not constant over the course of the current-voltage curve. These same authors used hexaquo nickel ion as a means of "verifying" their equations. These equations predicted a doubling of the slope of the $\log ((i_d)_m - i_m)/i_m$ vs. E plot in the part corresponding to the portion of the current-voltage curve above $E_{1/2}$, and apparently the experimental curve followed this behavior. In this laboratory, however, it has been found very difficult to eliminate completely the pronounced nickel maximum, which in some cases does not become apparent until the curve is actually analyzed. The presence of a slight maximum would result in an increase in the slope of the log

plot. In addition, it has not been adequately demonstrated in the literature that a Sargent Model XXI polarograph, which these same authors used, is capable of obtaining true current-voltage curves.

Mechanisms of Electroreduction.

Any mechanism proposed for electroreduction at the dropping mercury electrode must be consistent with the activation energies measured experimentally. Models representing the mechanism can yield activation energies, but considerable inaccuracy is introduced into the calculation. The more obvious faults of the mechanism can be seen, however. The steps in the reaction $M_{aq}^{n+} + ne^- = M_{Hg}$ that all complete mechanisms must include are, (1) the reducible species must be transported up to the electrode; (2) reduction electrons must be introduced into the species; (3) waters of hydration or complexing groups must be removed from the species; (4) the species must be transported across the electrical double layer at the electrode surface; (5) the metal atom must be dissolved in the mercury of the electrode. The only part of the total mechanism to which the experimental activation energies give a clue is the rate-determining step of the reaction. The other parts of the mechanism must only be consistent with the rate-determining step.

Two groups of mechanisms for electroreduction are possible. The first group contains the adsorption, desorption, and double-layer mechanisms. The adsorption mechanism requires that the reducible species be physically adsorbed on the electrode surface before any electrons can be transferred. For an aquo ion it is possible to picture the loss of one of the waters of hydration to allow the formation of a bond between the ion and metal atoms on the electrode surface. This would probably require considerable expenditure of energy, for the energy of bond

formation with the surface might not make up for the energy needed to split the water-ion bond. This mechanism would also include the case of a completely hydrated ion adsorbed on the surface.

The desorption mechanism for reduction to the metal requires that the slow step be the incorporation of an adsorbed ion into the electrode. The waters of hydration presumably would be removed at the same time as electrons are reducing the ion and probably would be the slow step.

Some authors consider the electrical double layer as a potential barrier which a reducible species must cross before it can be reduced. The activation energy in this mechanism would be the energy required to cross this barrier. The activation energy here might depend on the ions comprising the electrical double layer.

In the second group, the electron-transfer mechanism assumes that a reducible species can actually be reduced, or partially reduced, before it reaches a site on the electrode surface. According to Gurney,¹⁶ an electron has a finite probability of tunneling some distance away from the electrode surface. In terms of quantum mechanics, the wave function for the electrons in the metal electrode does not go abruptly to zero at the electrode surface, but has a finite amplitude out in the solution. The wave function of the electrons in the electrode may interact with the wave function of the reducible species and build up to an appreciable amplitude in the interior of the species. This amplitude represents the probability of capturing an electron before the species has actually reached the electrode surface. Again following Gurney,¹⁶ the total reduction current can be represented by two parts, $i_{\text{total}} = i_{+} + i_{e}$, where i_{+} is the current from the reduction of species that reach the electrode surface, and i_{e} is the current from reduction before the species arrives

at the electrode surface. Overvoltage raises the energy levels of electrons in the electrode relative to an ion in solution, and thus builds up a larger amplitude of the wave function for the transfer of electrons to the ion. This will favor the increase of i_e at the expense of i_+ .

Experimental Systems.

The dipositive ions of iron, cobalt, and nickel have many similarities and are all irreversibly reduced at the dropping mercury electrode. If the factors which determine the electrode kinetics are nearly the same, then many equivalences should be observed in the experimental data. The similarities should reduce some of the inherent inaccuracies in the method of evaluation of the mechanism of the electroreduction reactions. If the kinetics and mechanisms are not found to be the same in the three cases, perhaps the factors determining the kinetics can still be elucidated.

Cobalt and nickel metals are known to be soluble in mercury. Kolthoff and Lingane³² are of the opinion that elemental iron is not soluble. Bates and Fletcher,¹⁷ however, have prepared iron amalgams as high as 0.497% by weight by electrolysis for magnetic studies, indicating an appreciable solubility. Also, Tamman and Arntz¹⁸ found that mercury wets well on a clean solid alpha-iron surface in a vacuum. The evidence indicates that iron too is soluble in mercury.

Effects that may be useful in studying the mechanism of electroreduction are the complexing of the ion and adsorption of substances on the mercury surface. Sodium perchlorate is commonly used as a non-complexing medium, and was used as the inert electrolyte in the study of the aquo ions. Since Silverman and Dodson found a considerable increase in the electron exchange rate between ferrous and ferric ions when

chloride was present,¹⁹ sodium chloride was used as electrolyte in another series of studies. The sodium salt was chosen so that the same ion would comprise the solution side of the electrical double layer in both the complexing and non-complexing media. Agar has a pronounced effect on the surface tension, indicating that it is strongly adsorbed on a mercury surface. If the ions are reduced through the adsorption or desorption mechanisms, then agar in the solution should retard the rate of reduction. Goldberg and Jura²⁰ found little change in the surface tension of mercury in solutions containing more than 0.005% by weight agar, so that solutions with 0.01% agar were used.

Method of Interpretation of the Experimental Data.

(1) αn . When the value of αn is greater than unity, two electrons must be involved in the rate-determining step of the electrode reaction. When αn is less than one, n may be either one or two. The choice between the two must be made on the basis of the energies of activation.

(2) T . 25.0°C is the reference temperature for this study.

(3) K . Since there is no way of evaluating the transmission coefficient K , it will be assumed to be unity. It is recognized that in the electron-transfer mechanism, K could be very much less than unity.

(4) μ . Grahame⁸ in his studies on the capacity of the electrical double layer found that, in general, at a distance of 10 Å into the solution the potential had dropped to 90% of its initial value. Thus 10 Å seems to be the maximum distance at which an ion could be reduced, and will be used at first as the value of μ . Since this factor is included in a logarithmic term, small changes in the value of μ do not appreciably alter the energies of activation. Once a value of α is chosen, it can be used to estimate μ as the distance where the applied potential has fallen to αE .

(5) D. Diffusion coefficients, D , are calculated from the exact expression for the diffusion current given by Koutecky.

(6) ΔS^* . Powell and Latimer²² correlated aqueous entropies of ions as a function of charge, Z , effective radius of the ion, r_e , and atomic weight, M , in the equation

$$\bar{S}^0 = (3/2) R \ln M + 37 - 270 Z/r_e^2. \quad (17)$$

The effective radius of a cation is taken as Pauling's crystal radius plus 2 Å. This equation can be used to investigate possible activated complexes where either the charge or radius, or both, are different from those of the normal ion.

(7) ΔH^* . Williams²³ correlated the heats of hydration of gaseous dipositive ions by the expression

$$-\Delta H' = 150 Z/r + 0.3 I_{O2} - 40/r^3, \quad (18)$$

where z is the charge on the ion, r is the crystal radius in Å, I_{O2} is the ionization potential in kilocalories corresponding to the removal of two electrons. The first term represents electrostatic interaction with the solvent, the second term covalent linking with the solvent, and the third term electrostatic repulsion. Taking crystal radii and heats of hydration of gaseous ions from Quill,²⁴ Williams found +5% agreement. This equation can be extended to include unipositive and tripositive cations if it is changed to

$$-\Delta H' = 75 Z^2/r + 0.3 I_{OZ} - 10 Z^2/r^3. \quad (19)$$

Calculated values are compared with those given by Quill in Table 1. Uncertain values are included in parentheses. Some of the radii and ionization potentials, as well as the heats of hydration, have probably changed since these data were published. The average deviation for the +1 and +2 ions is 8 kcal.

(8) ΔF^* . The free energy change for various processes can be estimated by combining the correlation equations of the ionic entropies and the heat of hydration of the gaseous ions. The following method can also be used, but will merely set a limit on the value of the free energy change. If the mechanism of the electroreduction of the dipositive ions of iron, cobalt, and nickel is the same, the same fraction of the free energy to go to the unipositive state may be involved. Limits on the potential between the metal and unipositive state, and the unipositive and dipositive states can be set because the unipositive ions are not found when the metal is in contact with the dipositive ions. For M^+ to exist in a concentration of less than 0.1% of a 0.1 M solution of M^{++} , $K \geq 10^7$ for the reaction $2M^+ = M^{++} + M$. Therefore $E^0 \geq 0.42$. From this value Table 2 can be developed.

Table 1

Observed and Calculated Values for the Heat of Hydration of Gaseous Ions				
Ion	Crystal Radius A	Ionization Potential (kcal)	$-\Delta H'_{\text{obs}}$ (kcal)	$-\Delta H'_{\text{calc}}$ (kcal)
Li ⁺	0.71	124.3	125.4	114.8
Na ⁺	0.95	118.4	99.5	103.7
K ⁺	1.33	100.0	79.4	82.2
Rb ⁺	1.47	96.3	75.4	76.7
Cs ⁺	1.74	89.8	68.2	68.1
Cu ⁺	0.93	178.0	139.2	101.5
Ag ⁺	1.21	174.6	116.1	107.5
Tl ⁺	1.59	141	80	86.8
Mg ⁺²	0.66	523	464	471
Ca ⁺²	0.99	414	382	382
Sr ⁺²	1.15	385	350	350
Ba ⁺²	1.37	350	316	316
Ra ⁺²	1.50	355.5	311.7	295
Ti ⁺²	(0.85)	471	426	434
V ⁺²	(0.82)	483	453	441
Cr ⁺²	(0.80)	541	460	468
Mn ⁺²	0.78	531.7	444.7	460
Fe ⁺²	0.76	555.6	467.9	467
Co ⁺²	0.74	583	497	483
Ni ⁺²	0.73	596	507	490
Pd ⁺²	(0.85)	651	505	488
Cu ⁺²	(0.72)	645.6	507.2	507

(continued)

Table 1
(-2-)

Observed and Calculated Values for the Heat of Hydration of Gaseous Ions

Ion	Crystal Radius A	Ionization Potential (kcal)	$-\Delta H'_{\text{obs}}$ (kcal)	$-\Delta H'_{\text{calc}}$ (kcal)
Zn ⁺²	0.72	630.5	491.5	491
Cd ⁺²	0.96	597.0	436.5	444
Hg ⁺²	1.10	672.8	440.9	444
Sn ⁺²	1.10	506.3	373.5	389
Pb ⁺²	1.27	517.7	359.3	369
Al ⁺³	0.52	1227.6	1121.6	1029
Sc ⁺³	0.81	1022	958	971
Y ⁺³	0.96	911	786	874
La ⁺³	1.16	834.8	793.1	774
Ti ⁺³	0.64	1105	988	1043
V ⁺³	0.69	1094	970	1032
Cr ⁺³	0.62	1259	1093	1088
Mn ⁺³	0.66	1328	1111	1108
Fe ⁺³	0.64	1261	1059	1089
Co ⁺³	0.63	(1365)	1141	1120
Ga ⁺³	(0.60)	1319	1124	1103
In ⁺³	0.81	1214.5	994.6	1030
Tl ⁺³	0.95	1299	984	996

Table 2

Limiting Potentials for the Reactions $\underline{M} = M^+ + e^-$ and $M^+ = M^{++} + e^-$
at 25.0°C

Ion	$\underline{M} = M^+ + e^-$	$M^+ = M^{++} + e^-$	$\underline{M} = M^{++} + 2e^-$
Fe ⁺⁺	< + 0.23	> + 0.65	+ 0.44
Co ⁺⁺	< + 0.067	> + 0.487	+ 0.277
Ni ⁺⁺	< + 0.04	> + 0.46	+ 0.25

Since $\Delta F_{\text{form}} = \Delta F_{\text{sub}} + \Delta F_{\text{ion}} + \Delta F_{\text{hyd}} + \text{constant}$ for the reaction $\underline{M} = M^{n+} + ne^-$ in solution, the free energy of hydration difference between the dipositive and unipositive ions can be estimated. ΔF_{form} is the free energy of formation of the aqueous ion from the metal, ΔF_{sub} is the free energy of sublimation of the metal, ΔF_{ion} is the free energy of ionization, and ΔF_{hyd} is the free energy of hydration of the gaseous ion. The constant has the value -108.9 kcal and arises from the arbitrary convention that the free energy change is zero in the reaction $1/2 H_2 = H^+ + e^-$. $\Delta F_{\text{form}}^{1-2}$ is found from the potential for the reaction $M^+ = M^{++} + e^-$ using the relation $\Delta F = -nFE$. $\Delta F_{\text{sub}}^{1-2} = 0$. $\Delta F_{\text{ion}}^{1-2}$ is assumed to be the ionization potential for the second electron. $\Delta F_{\text{hyd}}^{1-2}$ is the free energy difference between the dipositive and unipositive states. The values calculated for $\Delta F_{\text{hyd}}^{1-2}$ are included in Table 3, along with those estimated from the correlation equations. The radii of the unipositive ions were assumed to differ from the radius of cuprous ion by the same amount that the dipositive ion differs from cupric.

Table 3

Free Energy, Heat, and Entropy Differences of Hydration of +1 and +2 Ions

at 25.0°C

Ion	$\Delta F_{\text{limiting}}^{1-2}$ (kcal)	$\Delta F_{\text{corr}}^{1-2}$ (kcal)	$\Delta H_{\text{corr}}^{1-2}$ (kcal)	$\Delta S_{\text{corr}}^{1-2}$ (eu)
Fe ⁺⁺	> 278	337	349	40.4
Co ⁺⁺	> 301	349	361	41.0
Ni ⁺⁺	> 322	357	369	41.4

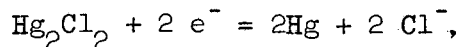
EXPERIMENTAL

Apparatus.

(1) A Heyrovsky Polarograph, Model XII, manufactured by E. H. Sargent and Co., was used to record the current-voltage curves. This polarograph utilizes a light-beam galvanometer that records on photographic paper mounted on a rotating drum. The galvanometer sensitivity was 7.58×10^{-3} microampere per millimeter.

(2) The dropping mercury electrode was made of Corning marine barometer tubing about 0.05 mm in diameter and 11.5 cm long. The drop-rate was controlled by raising or lowering a leveling bulb containing mercury. For this study the height of the mercury column was maintained at 85.5 cm above the tip of the capillary. The capillary constants were determined by timing the fall of 25 or 50 drops, and collecting and weighing them. With this electrode m was 1.37 mg sec^{-1} and t was 4.9 ± 0.4 sec throughout the range of temperature and voltage studied.

(3) Three reference saturated calomel electrodes (SCE) were prepared by grinding calomel with mercury and covering the mixture with a saturated KCl solution and excess solid KCl crystals. The electrodes were heated in a water bath to a temperature higher than that at which they were to be used and then allowed to cool in a constant-temperature bath. The constant-temperature bath was maintained at the desired temperature to within 0.1°C . The reference cells agreed with each other to within 4 millivolts at all temperatures. The potential of the SCE at the higher temperatures was corrected to 25°C by the known temperature coefficient. For the cell reaction,



$$\Delta E / \Delta T = 0.00025 \text{ volt } / ^{\circ}\text{C}^{\cdot 31}$$

$$E^{\circ} = + 0.242 \text{ volt vs. NHE.}$$

Liquid junction potentials were neglected.

(4) The electrolytic cell was of the H-type, with a fine sintered glass disk and an agar plug separating the two compartments. In the experiments where the absence of chloride ion was desired, an agar plug made by dissolving 3.6 g of Bacto-Agar in 100 ml of hot 0.1 N NaClO_4 was used. Here the anode consisted of a mercury pool covered by a solution of mercurous nitrate in 0.1 N NaClO_4 . With 0.1 N NaCl as supporting electrolyte, the anode was a 0.1 N calomel electrode. Two salt bridges made from glass tubing and Tygon tubing connected the cathode compartment with the SCE. The bridge inserted in the cathode compartment was filled with agar-gel containing the supporting electrolyte being used. The second bridge was filled with agar-gel containing saturated KCl. The two bridges were interconnected by a bottle containing saturated KCl.

(5) The potential of the dropping mercury electrode referred to the SCE was measured by a Rubicon student potentiometer. At first a G. E. recording potentiometer was used to measure the potential continuously throughout the current-voltage curve. The current drawn by this instrument, however, was found to deflect the galvanometer of the polarograph. This resulted in a distortion of the current-voltage curve and in some cases the apparent measured potential differed from the true value by as much as 0.05 volt.

The potential axis of the current-voltage curve was calibrated at a certain potential by flashing a light inside the polarograph case, which registered as a line on the photographic paper. This line was found to differ from the position of the galvanometer light beam at that potential. Since the photographic paper on the drum is not flush

against the shutter of the camera, the position of the line will depend upon the position of the source of light inside the case. The final method evolved was to record the potential at the start and finish of a current-voltage curve, and to put on potential lines at the same time. The potential lines were calibrated by using the points at the start and finish of each curve. The number of volts per millimeter was then determined by the distance between the two lines.

(6) The current axis was calibrated by placing a standard resistor in place of the electrolysis cell and measuring the deflection of the galvanometer as a function of the applied potential. The total resistance of the circuit is composed of the standard resistance plus the resistance of the galvanometer and the Fisher-Ayrton shunt.

Reagents.

All stock solutions were made up from C.P. chemicals and distilled water.

(1) Nickel perchlorate solutions were made by dissolving the salt in distilled water with sufficient HClO_4 so that dilution would produce the desired pH for the experiments. The solution was standardized by the cyanide method after the AgNO_3 was previously standardized versus NaCl .

(2) Cobaltous perchlorate solutions were made up and standardized in a similar fashion, using the procedure given by Kolthoff and Stenger.²⁵

(3) Ferrous solutions were made by dissolving ferrous ammonium sulfate of known purity in a solution 0.001 normal in HClO_4 . Since ferrous ion is slowly oxidized by air in slightly acid solutions, a fresh solution was prepared for each set of experiments.

(4) All supporting electrolytes were prepared by dissolving the

solid salts in distilled water and diluting up to volume.

(5) A solution of agar was prepared by dissolving Difco Bacto-Agar in boiling water and placing in a hot water bath at 90°C for an hour. This precaution was taken to insure the complete and uniform hydrolysis of the agar. Fresh solutions were prepared for each set of experiments.

Experimental procedure.

A quantity of the standard solution was pipetted into a volumetric flask, the proper amount of solid salt or solution of supporting electrolyte was added, and the solution was made up to volume. The ions were studied in three media: (1) 0.1 N NaClO₄ and 0.0001 M La(NO₃)₃; (2) 0.1 N NaCl and 0.0001 M La(NO₃)₃; (3) 0.1 N NaClO₄ and 0.01% by weight agar. The ions were in a concentration of 0.0005 M. Dissolved oxygen was removed from the solution by bubbling purified nitrogen (purified over copper at 400°C) through the solution for 30 minutes. The dropping mercury electrode was washed while running by dipping alternately in concentrated nitric acid and distilled water. Two current-voltage curves for each solution were recorded.

Precision and accuracy of the data.

The diffusion coefficients of the aquo ions were calculated from the exact expression for the diffusion current, Eq. (6), with the constant A given the value of 34. Values obtained at 25°C with 0.1 N NaClO₄ as supporting electrolyte are

$$D_{Ni^{++}} = 5.84 \times 10^{-6} \text{ cm}^2/\text{sec},$$

$$D_{Co^{++}} = 5.71 \times 10^{-6} \text{ cm}^2/\text{sec},$$

$$D_{Fe^{++}} = 5.68 \times 10^{-6} \text{ cm}^2/\text{sec}.$$

The value of the diffusion coefficient of nickelous ion is in good agreement with that experimentally determined, $D_{Ni^{++}} = (6.0 \pm 0.6) \times 10^{-6} \text{ cm}^2/\text{sec}$

in 0.1 N NaClO₄.²⁶ According to the macroscopic diffusion coefficient data of Ohlm,²⁷ the diffusion coefficient of cobaltous ion should be close to that of nickelous. The variation of the diffusion coefficient with supporting electrolyte was insignificant.

Half-wave potentials ($E_{1/2}$) were obtained with a precision of 4 millivolts, which is the variation observed in the SCE reference cells. Experimental values were found to vary at most by this amount. In a control experiment, $E_{1/2}$ for thalious ion was 0.453 ± 0.004 volts vs. SCE as compared to the literature value of 0.460 ± 0.005 volts.²⁸

The limiting factor in the complete analysis and interpretation of the data was found to be in obtaining precise values of αn . The prominent nickel maximum persisted to a slight degree even when La(NO₃)₃ was present as a maximum suppressor. Consequently, only the lower portion of the current-voltage curve was used to obtain the value of αn . With agar serving as the maximum suppressor, the maximum was completely eliminated. In many of the $\log (i_d - i)/i$ plots of cobaltous and ferrous ions considerable non-linearity at the extremes of the plot was observed. The central portion of the plot is the most accurate, and was used to evaluate αn . Values of αn are reported to ± 0.02 , but in some cases are actually more precise than this. The variation in αn may be caused by impurities in the solution that could be eliminated by the use of conductivity water in place of distilled water. Many more points for the log plots could be obtained by reducing the rate of polarization of the electrode from the 2.67 mv/sec that was used to about 1 mv/sec. This could be accomplished by inserting an auxiliary battery into the circuit and reducing the voltage applied to the rotating bridge. The rate of polarization of the electrode

used may be partly responsible for the non-linearity of the log plots. The assumption necessary for the use of recording polarographs is that even though the degree of polarization is changing, the response of the instrument introduces no distortion of the current-voltage curves. In general, recording polarographs of the type used here produce results identical to those obtained manually. In cases where extreme accuracy is required, however, current-voltage curves should be determined manually.

Experimental Results and Interpretation.

The current-voltage curves. Typical current-voltage curves obtained with the three ions in the three media are shown in Figs. 3-5. The curves are arbitrarily placed on the potential axis. The curve represents the average of the observed galvanometer oscillations. Only the curves of nickelous ion gave good diffusion current plateaus. In many of the curves of cobaltous and ferrous ions the diffusion current plateau was obscured by a rise in current that was not reproducible. The rise was independent of maximum suppressor used.

Plots of $\log (i_d - i)/i$ vs. $-E$ are presented in Figs. 6-8. These plots correspond to the current-voltage curves depicted in Figs. 3-5. The effect of the nickel maximum is clearly evident in Figs. 6 and 7. The non-linearity of the log plots of cobaltous and ferrous ions at the higher temperatures was in general greater than that at 25.0°C.

Experimental values of the half-wave potentials and αn are given in Tables 4-6.

The activation energies. Values of $E_{1/2}$ vs. the "rational potential" (ECM) and the NHE were calculated using the relations

$$E_{1/2} (\text{ECM}) = E_{1/2} (\text{SCE}) + 0.439,$$

$$E_{1/2} \text{ (NHE)} = E_{1/2} \text{ (SCE)} + 0.242.$$

Plots of $-\alpha n E_{1/2}$ vs. temperature are shown in Figs. 9-11. In the case of nickelous ion in 0.1 N NaCl, αn was taken as the average of all the values at the various temperatures, $\alpha n = 0.872$. The data were fitted to straight lines by the method of least squares. The lines may be represented by the equation $-\alpha n E_{1/2} = a_2 + bT$, where a_2 and b are constants, and T is the absolute temperature. The quantity $a_2 = \Delta H^*/F$, and is the intercept at 0°K . The slope $b = -\Delta S^*/F - (R/F) \ln \cdot 0.87 (kT/h) K \mu (t/D)^{1/2}$. The intercept of the line at 25°C yields $-\alpha n E_{1/2}^{25^\circ}$. The plots for cobaltous ion in agar solution and ferrous ion in all three solutions were not fitted because of the extreme scatter in the data. If the data had been analyzed and the results interpreted, negative heats of activation would result. Values of $\Delta F^*_{25^\circ}$ can be calculated from the observed values of $-\alpha n E_{1/2}$ at 25°C , however. The scatter in these latter data is probably caused by a change in the nature of the species undergoing the electrode reaction. Since the wave due to hydrogen ion reduction would interfere with the cobaltous and ferrous waves if the pH were low, the acid concentration was made only ca. 5×10^{-6} N. The first hydrolysis constants for the three ions at 25.0°C are

$$K_{\text{Fe}^{++}} = 5 \times 10^{-9},^{29}$$

$$K_{\text{Co}^{++}} = 6.3 \times 10^{-13},^{30}$$

$$K_{\text{Ni}^{++}} = 2.3 \times 10^{-11},^{30}$$

The nickel solutions were made 0.001 M in HClO_4 , so that hydrolysis at any of the temperatures was probably negligible. The hydrolysis of cobaltous ion was also probably negligible in view of the low value of the hydrolysis constant. At 25°C in the solution used, ferrous

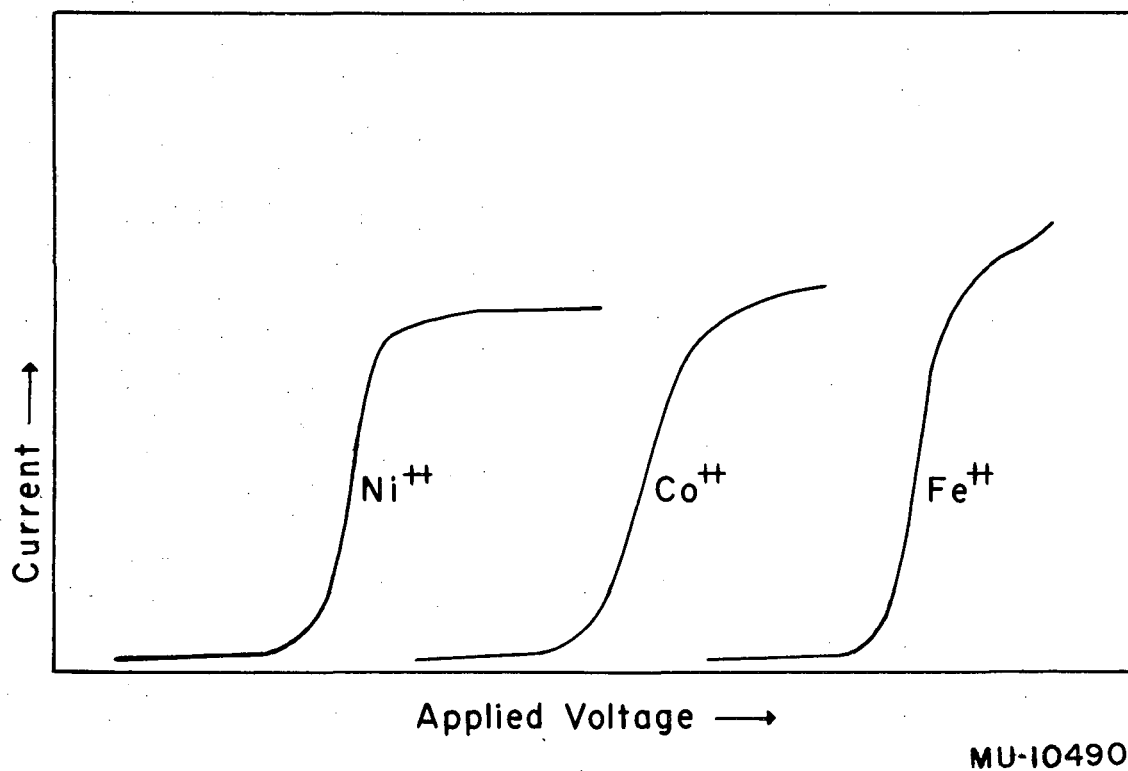
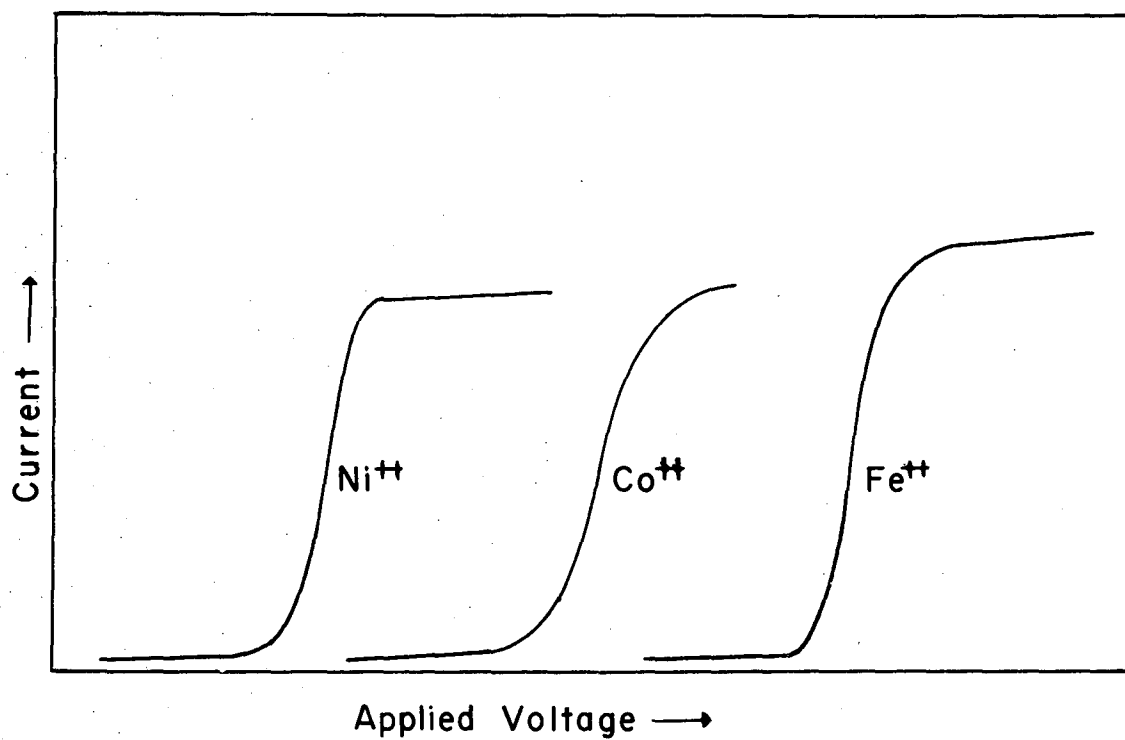
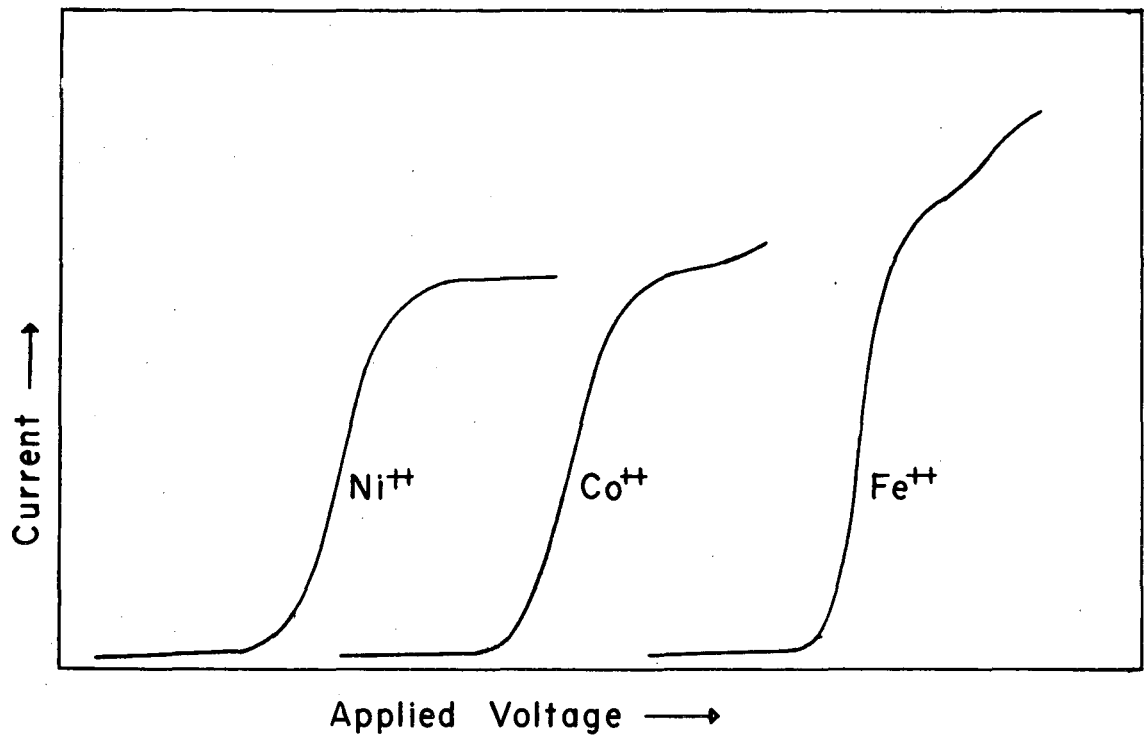


Fig. 3. Typical current-voltage curves for the reduction of nickelous, cobaltous and ferrous ions at 25.0 °C. in 0.1 M NaClO₄.



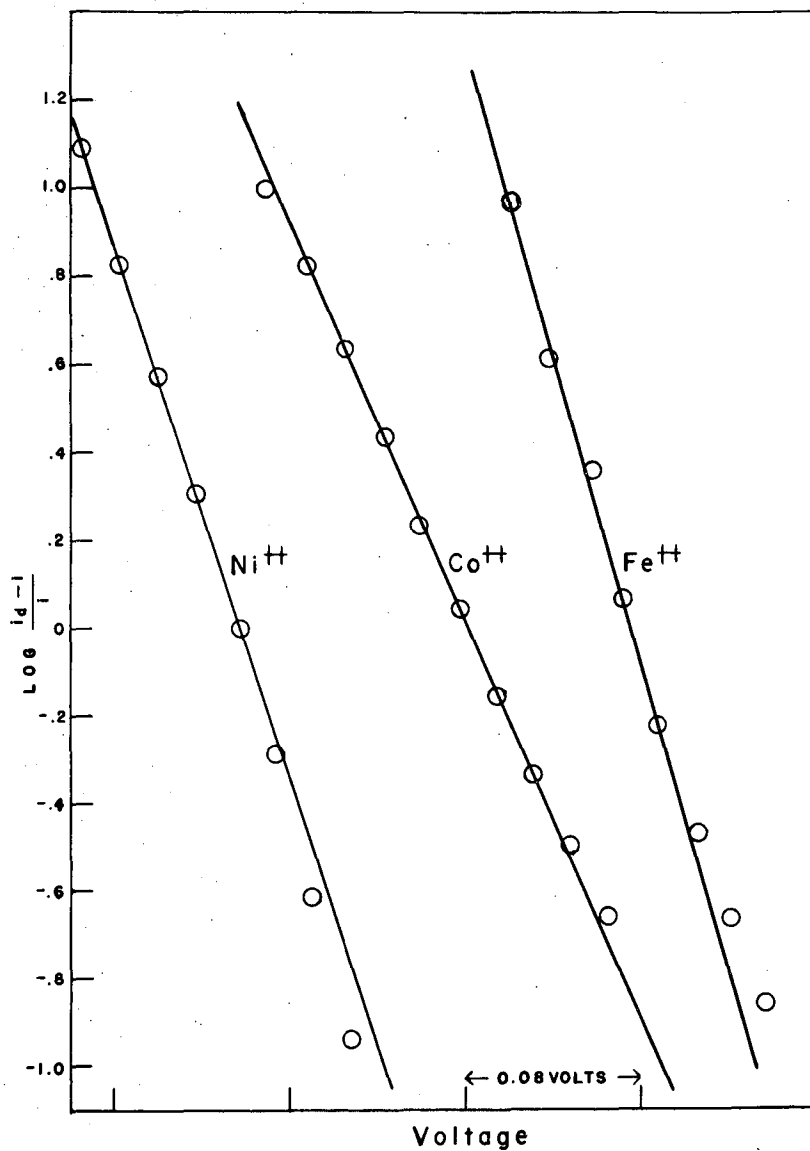
MU-10491

Fig. 4. Typical current-voltage curves for the reduction of nickelous, cobaltous and ferrous ions at 25.0 °C. in 0.1 M NaCl.



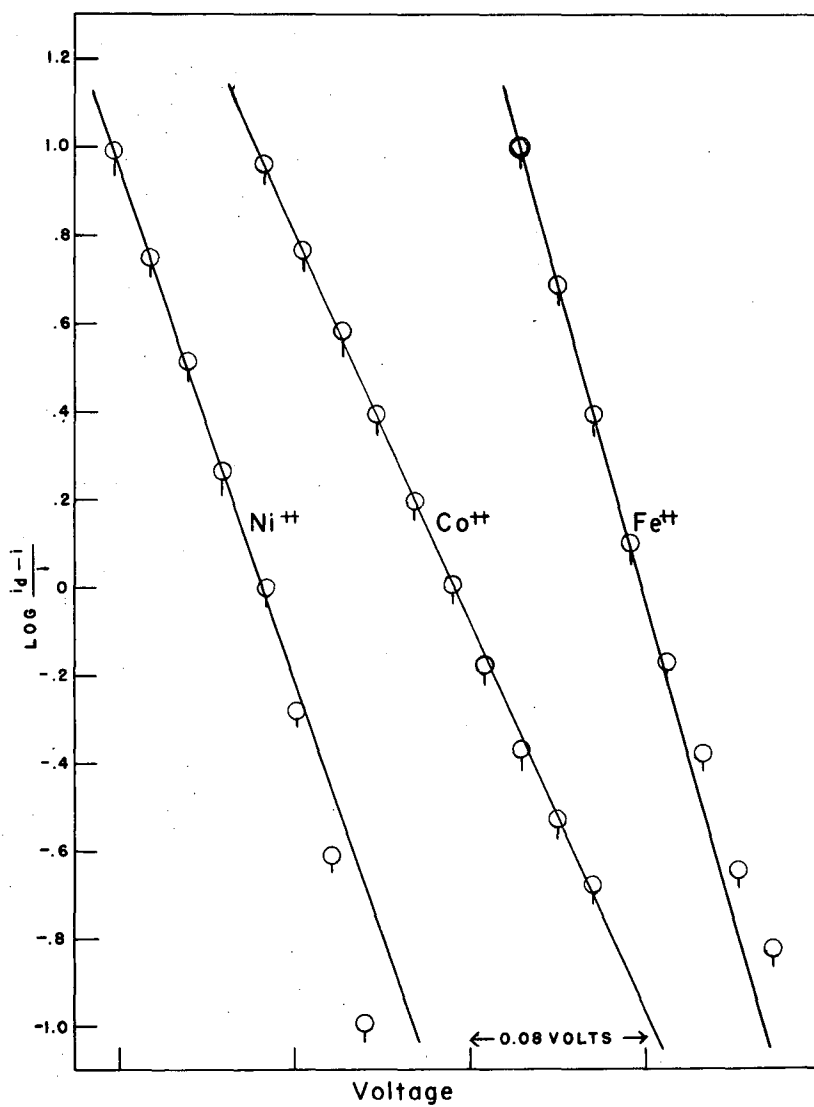
MU-10492

Fig. 5. Typical current-voltage curves for the reduction of nickelous, cobaltous and ferrous ions at 25.0 °C. in 0.1 M NaClO₄ and 0.01% agar.



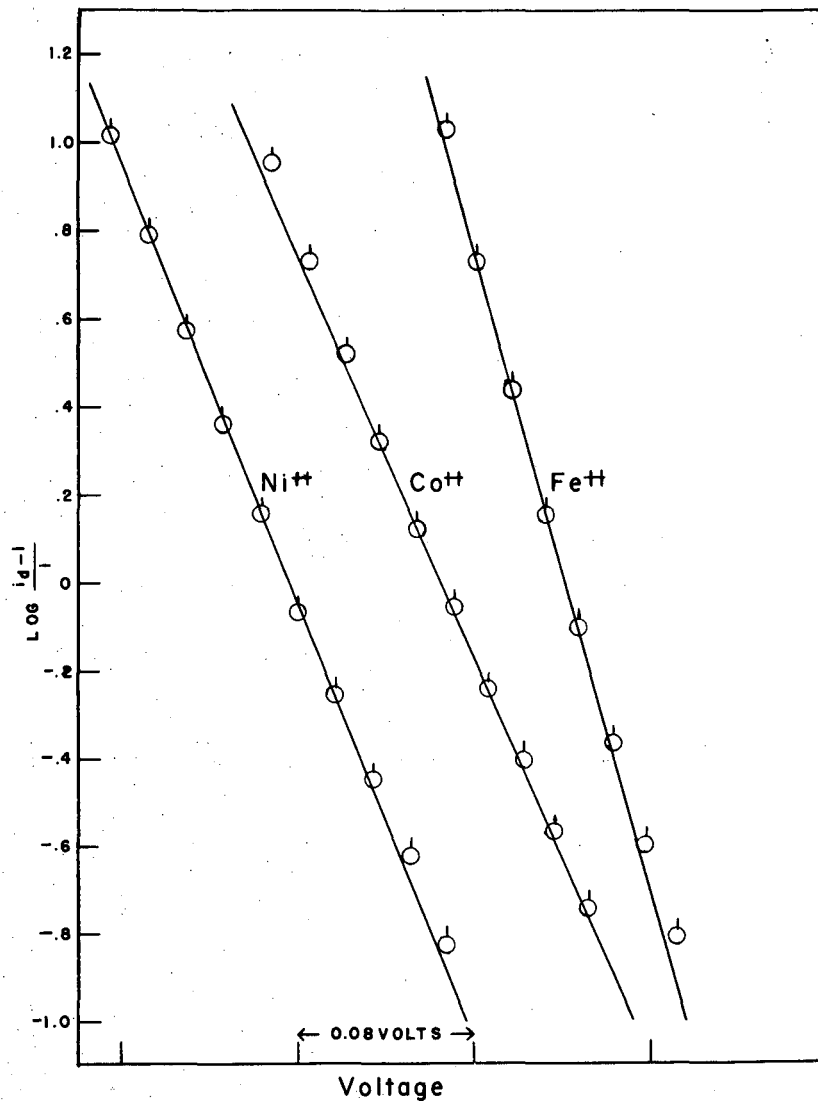
MU-10493

Fig. 6. $\text{Log } \frac{i_d - i}{i}$ vs. potential plot for nickelous, cobaltous and ferrous ions at 25.0 °C. in 0.1 M NaClO_4 . The plots apply to the current-voltage curves in Fig. 3.



MU-10494

Fig. 7. $\log (i_d - i)/i$ vs. potential plot for nickelous, cobaltous and ferrous ions at 25.0 °C. in 0.1 M NaCl. The plots apply to the current-voltage curves in Fig. 4.



MU-10495

Fig. 8. $\text{Log} \frac{i_d - i}{i}$ vs. potential plot for nickelous, cobaltous and ferrous ions at 25.0 °C. in 0.1 M NaClO_4 and 0.01% agar. The plots apply to the current-voltage curves in Fig. 5.

Table 4

 Experimental Values of the Half-wave Potential and αn in 0.1 N NaClO₄

Temperature °C	$-E_{1/2}$ vs. SCE (volts)	αn
A. Nickelous		
25.0	0.991	0.896
32.1	0.976	0.864
40.2	0.962	0.848
48.6	0.932	0.834
B. Cobaltous		
25.0	1.222	0.670
32.1	1.196	0.684
40.2	1.177	0.680
48.0	1.149	0.700
48.6	1.136	0.709
C. Ferrous		
25.0	1.296	1.044
32.1	1.292	1.062
40.2	1.279	1.229
48.0	1.268	1.238
48.6	1.262	1.218

Table 5

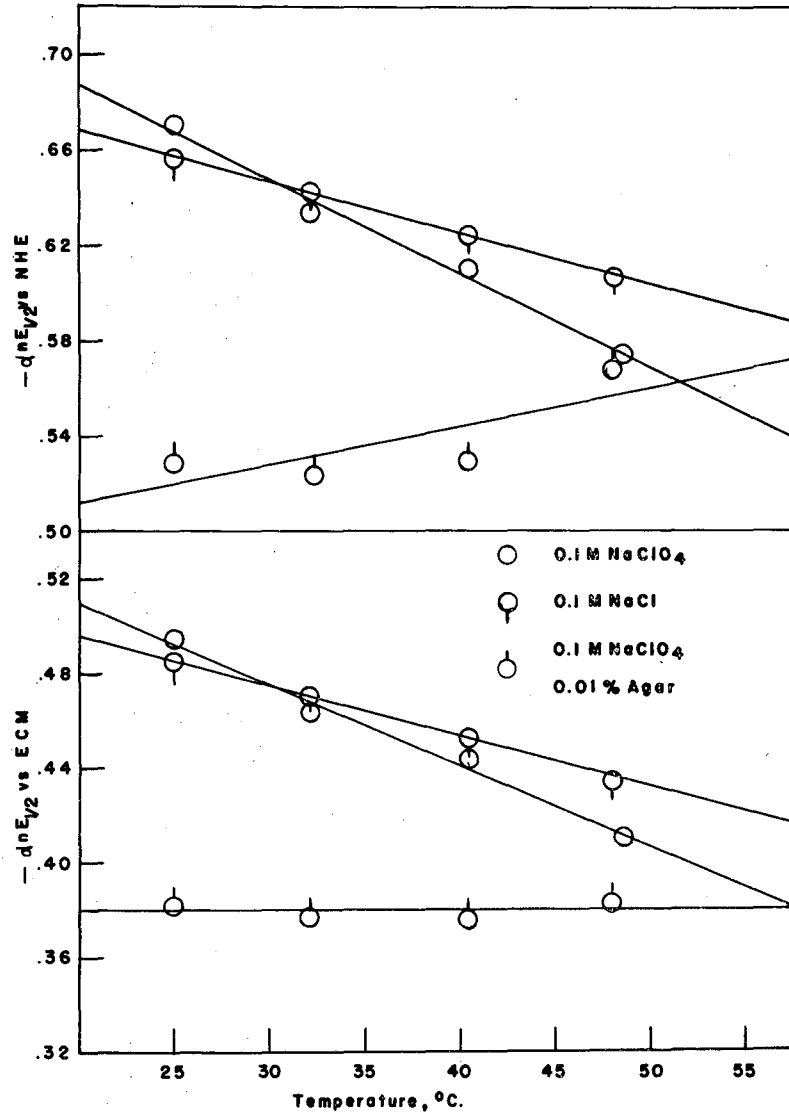
Experimental Values of the Half-wave Potential and αn in 0.1 N NaCl

Temperature °C	$-E_{1/2}$ vs. SCE (volts)	αn
A. Nickelous		
25.0	0.996	0.870
32.1	0.979	0.872
40.2	0.959	0.874
48.0	0.938	0.870
48.6	0.938	0.874
B. Cobaltous		
25.0	1.210	0.662
32.1	1.202	0.666
40.2	1.177	0.664
48.0	1.127	0.704
48.6	1.123	0.704
C. Ferrous		
25.0	1.298	1.077
32.1	1.295	1.114
40.2	1.283	1.213
48.0	1.271	1.190
48.6	1.271	1.228

Table 6

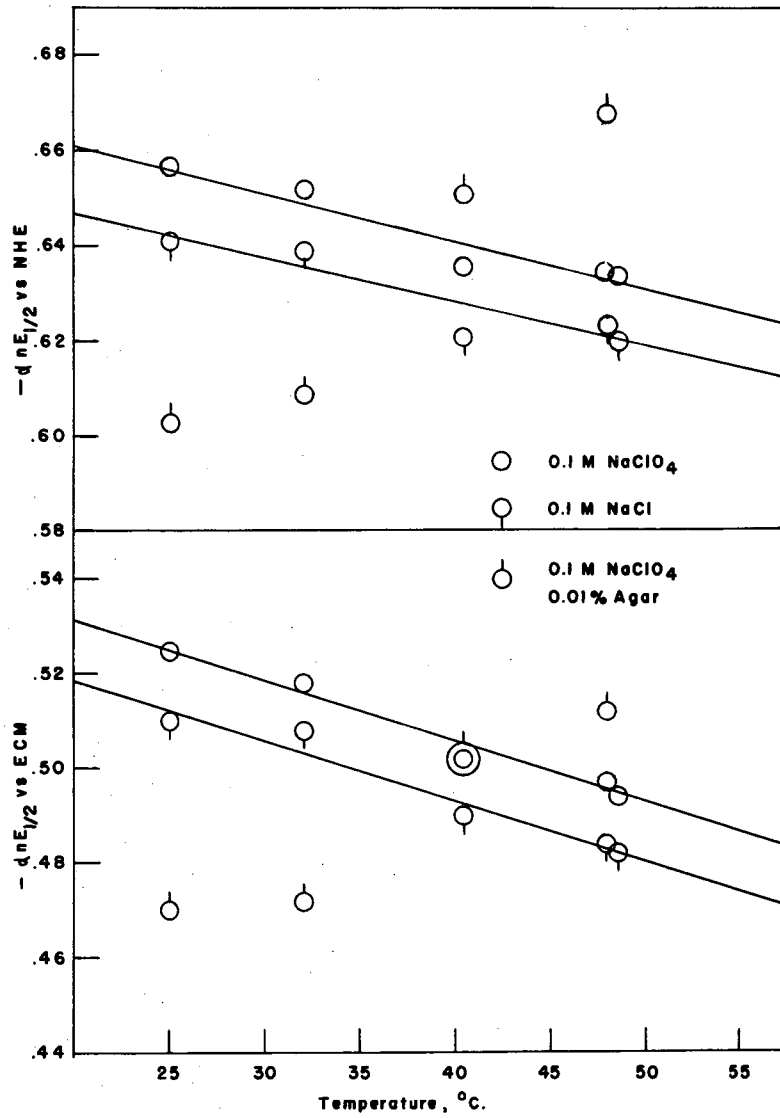
Experimental Values of the Half-wave Potential and αn in 0.1 N NaClO₄
and 0.01 % Agar

Temperature °C	$-E_{1/2}$ vs. SCE (volts)	αn
A. Nickelous		
25.0	0.953	0.744
32.1	0.946	0.744
40.2	0.920	0.782
48.0	0.848	0.937
B. Cobaltous		
25.0	1.132	0.678
32.1	1.115	0.698
40.2	1.106	0.753
48.0	1.086	0.792
C. Ferrous		
25.0	1.292	1.075
32.1	1.284	1.158
40.2	1.281	1.228
48.0	1.275	1.220
48.6	1.268	1.225



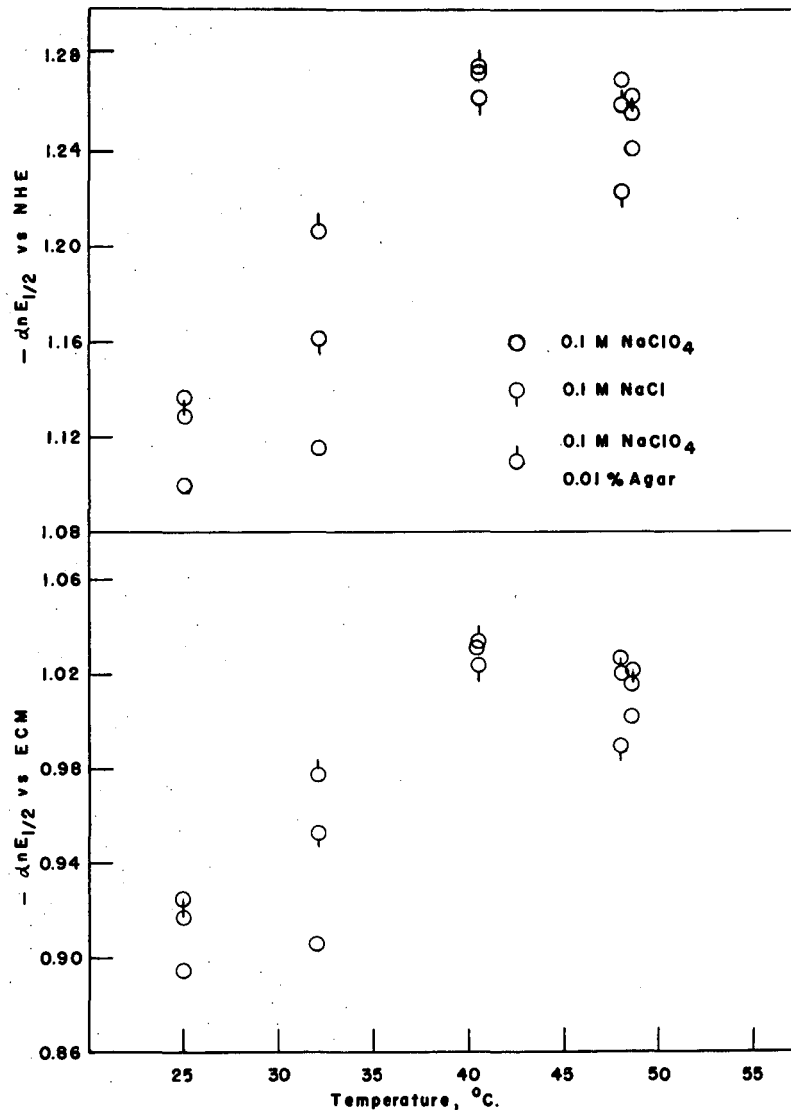
MU-10496

Fig. 9. Plots of $-anE_{1/2}$ vs. temperature for nickelous ion.



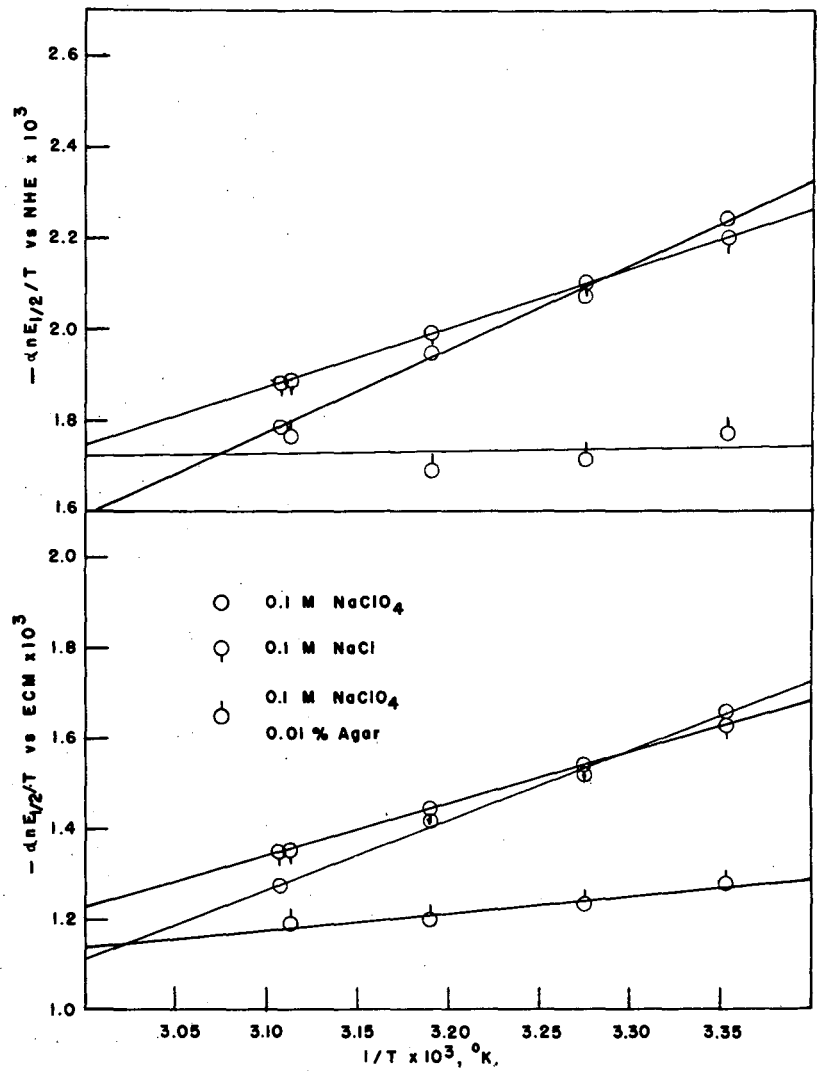
MU-10497

Fig. 10. Plots of $-dnE_{1/2}$ vs. temperature for cobaltous ion.



MU-10498

Fig. 11. Plots of $-\Delta nE_{1/2}$ vs. temperature for ferrous ion.



MU-10499

Fig. 12. Plots of $-anE_{1/2}/T$ vs. $1/T$ for nickelous ion.

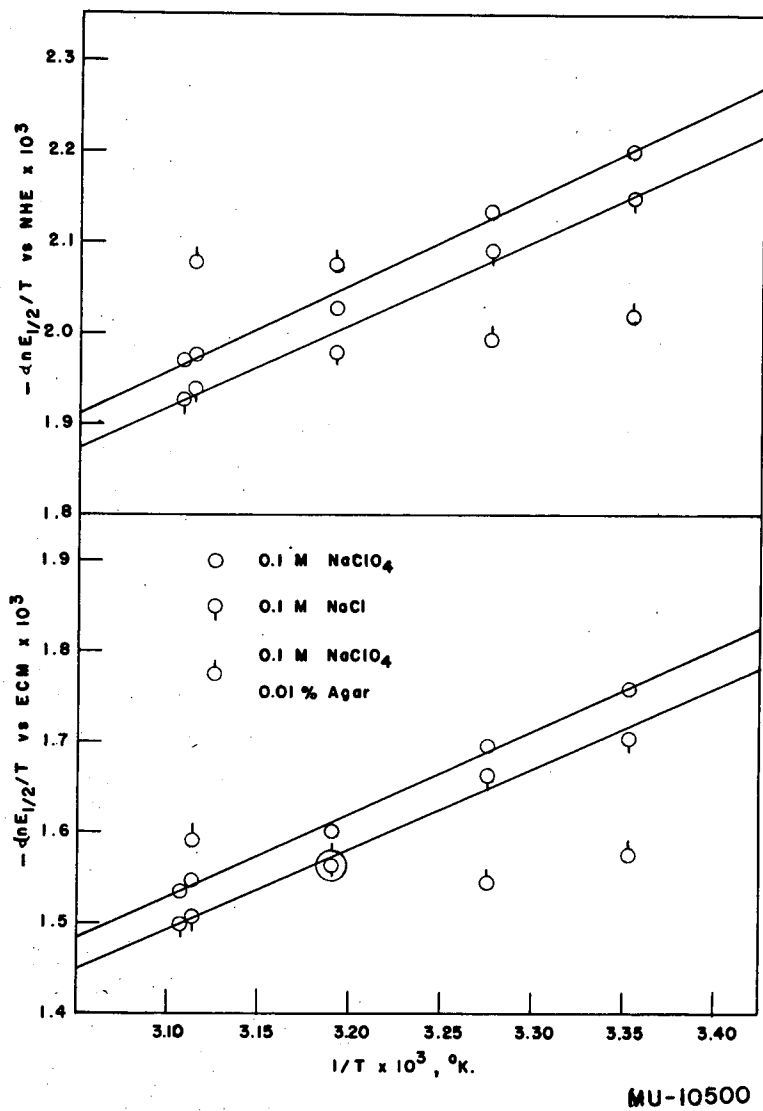


Fig. 13. Plots of $-dnE_{1/2}/T$ vs. $1/T$ for cobaltous ion.

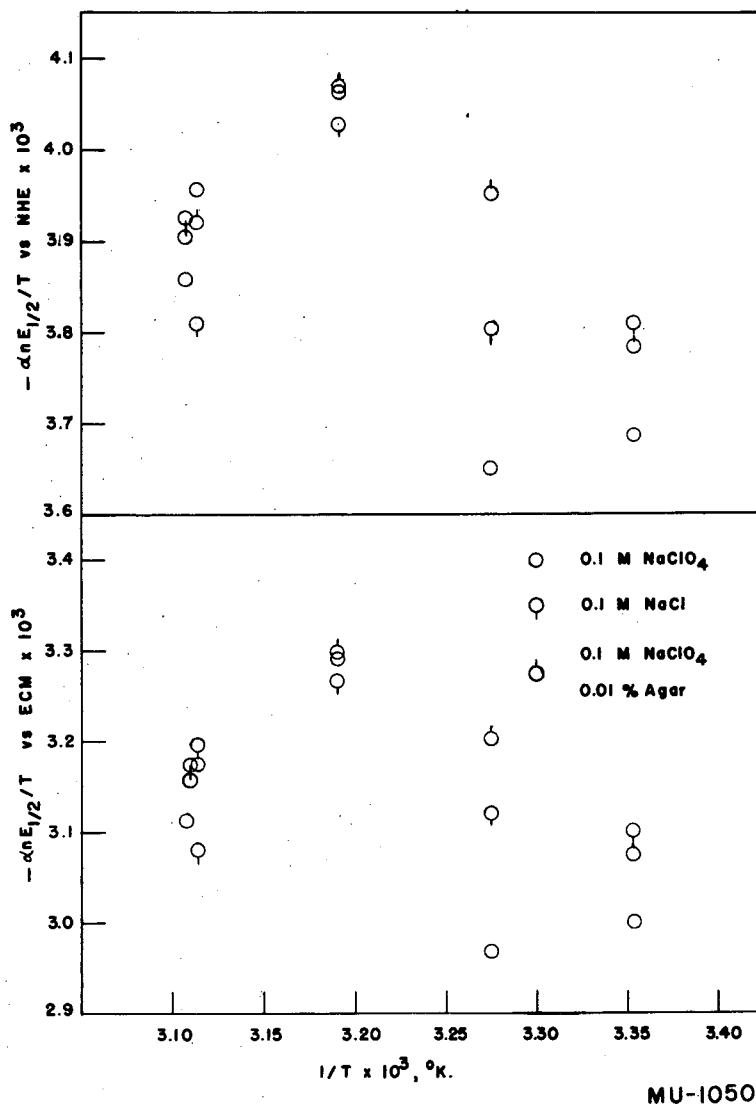


Fig. 14. Plots of $-anE_{1/2}/T$ vs. $1/T$ for ferrous ion.

MU-10501

Table 7

The Free Energy, Heat, and Entropy of Activation for the Reduction of Nickelous, Cobaltous, and Ferrous Ions to the Metals at 25.0°C in a Non-complexing Solution, 0.1 N NaClO₄

Quantity	Nickelous		Cobaltous		Ferrous	
	ECM	NHE	ECM	NHE	ECM	NHE
$-a_{1/2}^{25^{\circ}}$ (volts)	0.493	0.668	0.525	0.656	0.895	1.100
"b", mv/deg	-3.45	-3.95	-1.3	-1.0		
"a" ₁ , volts	1.546	1.839	0.917	0.963		
"a" ₂ , volts	1.522	1.846	0.913	0.955		
ΔF^* , Kcal	23.3	27.3	24.0	27.0	32.5	37.3
ΔH^*_1 , Kcal	35.7	42.4	21.1	22.2		
ΔH^*_2 , Kcal	35.1	42.6	21.0	22.0		
ΔS^* , e.u.	39.7	51.2	-9.9	-16.8		

Table 8

The Free Energy, Heat and Entropy of Activation for the Reduction of Nickelous, Cobaltous, and Ferrous Ions to the Metals at 25.0°C in a Complexing Solution, 0.1 N NaCl

Quantity	Nickelous		Cobaltous		Ferrous	
	ECM	NHE	ECM	NHE	ECM	NHE
$-\alpha n E_{1/2}^{25^\circ}$ (volts)	0.486	0.658	0.512	0.642	0.925	1.137
"b", mv/deg	-2.15	-2.15	-1.27	-0.92		
"a" ₁ , volts	1.150	1.300	0.889	0.922		
"a" ₂ , volts	1.142	1.314	0.891	0.916		
ΔF^* , Kcal	23.1	27.1	23.7	26.7	33.2	38.1
ΔH^*_1 , Kcal	26.5	30.0	20.5	21.2		
ΔH^*_2 , Kcal	26.3	30.3	20.5	21.1		
ΔS^* , e.u.	9.8	9.8	-10.6	-18.6		

Table 9

The Free Energy, Heat, and Entropy of Activation for the Reduction of Nickelous, Cobaltous, and Ferrous Ions to the Metals at 25.0°C in

0.1 N NaClO₄ and 0.01 % Agar

Quantity	Nickelous		Cobaltous		Ferrous	
	ECM	NHE	ECM	NHE	ECM	NHE
$-\alpha n E_{1/2}^{25^{\circ}}$ (volts)	0.380	0.520	0.470	0.603	0.917	1.129
"b", mv/deg	0.00	1.60				
"a" ₁ , volts	0.374	0.058				
"a" ₂ , volts	0.380	0.043				
ΔF^* , Kcal	20.7	23.9	22.7	25.8	33.0	37.9
ΔH^*_1 , Kcal	8.6	1.3				
ΔH^*_2 , Kcal	8.8	1.0				
ΔS^* , e.u.	-39.8	-76.7				

ion is negligibly hydrolyzed, but may very well be at the higher temperatures. The behavior of this ion definitely indicates that a new species is formed at the higher temperatures.

Plots of $-\alpha n E_{1/2}/T$ vs. $1/T$ are shown in Figs. 12-14. Again the data were fitted to straight lines by the method of least squares. The equation for the line $-\alpha n E_{1/2}/T = a_1/T + \text{constant}$, gives the value of the heat of activation, as the slope $a_1 = \Delta H^*/F$. In theory, a_1 should be equal to a_2 , which is the intercept of the $-\alpha n E_{1/2}$ vs. T plot at 0°K , but they may differ slightly because of the inaccuracy in plotting the experimental data. The plots for ferrous ion again clearly indicate that a different species is formed at the higher temperatures.

Values of $-\alpha n E_{1/2}^{25^\circ}$, "b", "a₁", "a₂" and the calculated activation energies are included in Tables 7-9 for the three supporting electrolytes.

The values of ΔF^* and ΔH^* are probably good to ± 1 kcal, while the probable error in ΔS^* is about 5 e.u. A recalculation of the thickness of the reaction layer, μ , with the knowledge of the value of α , would add at most 2 e.u. to ΔS^* .

The scatter in the data was noticeably less when the "rational potential" was used as the reference point for the electrode potential. This fact is at least an indication that the potential of the electrocapillary maximum of mercury in the absence of specific adsorption is the best approximation to a potential zero.

Mechanisms. Since the "rational potential" is considered to be a better reference point, only the activation energies calculated from this reference are discussed. Intercomparisons of the activation energies indicate clearly that the mechanism of electroreduction is not the same for the three ions. The difference might be explained

by the different nature of the aquo ions. Taube²¹ has recently written a review on complexes formed in aqueous systems. From kinetic studies on the rate of exchange of the complex with the media, the conclusion was reached that cobalt and nickel probably form outer-type (labile) water complexes, while ferrous ion might form an inert aquo complex. In comparing the exchange rates of cyanide, water, and ammonia, it has been found that water is intermediate between cyanide and ammonia. Cyanide forms a labile complex with nickel, and inert complexes with ferrous ion. Cobaltous may be inert, although in practice it is difficult to get a complex with a definite composition of cyanide. Ammonia definitely forms labile complexes with nickel and cobaltous, ferrous ion not being listed. Since the aquo complexes are more labile than those of cyanide, the aquo nickelous ion is definitely labile, that of cobaltous probably is, but that of ferrous ion may be inert.

Ratios of the experimental free energy of activation, ΔF^* , for the aquo complex at 25°C to the free energy of hydration difference between the dipositive and unipositive states, $\Delta F_{\text{limiting}}^{1-2}$, from Table 3 are 0.117, 0.0798, and 0.0724 for ferrous, cobaltous, and nickelous ions, respectively. If the correlation free energy difference is used instead, the ratios are 0.0965, 0.0680, and 0.0653 for the ions in the same order. If the reduction mechanism is essentially the same for all three ions, it might be expected that these ratios would be constant. On this basis the mechanism for the reduction of ferrous ion is different from that for either cobaltous or nickelous ions. The best evidence that the mechanisms for the reduction of cobaltous and nickelous ions are different is that the entropies of activation are widely at variance and are of opposite

sign.

(1) The reduction of nickelous ion. The experimental activation energies for the reduction of the pure aquo nickelous ion at 25°C are

$$\Delta F^* = 23.3 \text{ kcal.}$$

$$\Delta H_1^* = 35.7 \text{ kcal.}$$

$$\Delta S^* = 39.7 \text{ e.u.}$$

If the transmission coefficient K for nickelous ion were less than unity, ΔS^* would be more positive and ΔF^* would be smaller. The large positive value of ΔS^* rules out the adsorption mechanism since adsorption would result in a more ordered state than that of the normal ion. Agar adsorbed on the mercury surface does not retard the reduction of nickelous ion, which fact also makes the adsorption and desorption mechanisms unlikely.

In the electron transfer mechanism, the sphere of water molecules hydrating the nickelous ion would have to be rearranged to allow introduction of one or two electrons. Since the probability of the simultaneous introduction of two electrons would be much smaller in this mechanism than the introduction of one at a time, the rate-determining step probably involves the introduction of the first electron to form the unipositive state. The unipositive ion would be very rapidly reduced by the introduction of the second electron. The difference in energy between a nickelous ion and a nickelous ion with the water configuration of a plus-one ion can be calculated by using the correlation equations. Assuming a uniform spherical distortion of all the water molecules, the new radius of the nickelous ion would be that estimated for the unipositive state, 0.94 Å as compared to 0.73 Å for the normal nickelous ion. Neglecting any change in the ionization potential, a

heat difference of 37 kcal is calculated. The corresponding entropy change is 11 e.u. ΔS^* is practically identical with the value calculated for the difference between the dipositive and unipositive states, $\Delta S_{\text{corr}}^{1-2} = 41.4$ e.u. It is interesting that experimental activation energies are at least consistent with the hypothesis that the slow step in the reduction of the aquo nickelous ion is the formation of unipositive nickel. Thus, n is chosen as one and $\alpha = 0.896$. The site of reduction of the aquo nickel complex is then about 10 Å from the electrode surface.

The effect of chloride ion is to lower both ΔH^* and ΔS^* . At the present time there is no way of calculating expected energy changes for a complex with chloride, but the decrease in heat of activation from 35.7 kcal to 26.5 kcal is not inconsistent with the electron transfer mechanism. A complexed chloride ion might help to lower the energy required for the passage of an electron from the electrode to the ion. It would be expected instead that chloride ion would increase the transmission coefficient, K .

Agar in the solution also enhances the rate of reduction of nickelous ion. This is probably caused by the ion being complexed by the agar adsorbed on the mercury surface. It is known that, in general, replacing a complexed water molecule with a different complexing group increases the rate of oxidation-reduction reactions. Complexing groups such as chloride, or in this case agar, are perhaps a pathway of lower energy that the electrons follow. The low value of the entropy of activation may be caused by the complexing of the nickelous ion to a species that is physically adsorbed on the mercury surface, or in part by a smaller value of the transmission coefficient K .

(2) The reduction of cobaltous ion. The experimental activation energies for the reduction of the aquo cobaltous ion at 25°C are

$$\Delta F^* = 24.0 \text{ kcal,}$$

$$\Delta H^* = 21.1 \text{ kcal,}$$

$$\Delta S^* = -9.9 \text{ e.u.}$$

Although the entropy of activation is negative, the fact that agar increases the rate of reduction rules out the adsorption mechanism. A small value of the transmission coefficient K would increase ΔS^* . The non-linearity observed in the $\log(i_d - i)/i$ vs. $-E$ plots may be an indication that two different paths of reduction are competing with each other. To see whether or not this is actually the case, the current-voltage curves should be determined more accurately by reducing the rate of polarization of the electrode as outlined above. Extending the temperature range down to 0°C would also give needed information. If two paths are involved, then the calculated activation energies are the average for the two mechanisms. For the purposes of this discussion it is assumed that only one path is involved. The heat and entropy changes for the expansion of the hydration sphere are nearly the same as in the nickelous case. On the basis of these energies there is no way of deciding if the rate-determining step is the formation of the unipositive state. If two electrons were involved in the rate-determining step, then α would be 0.335. This would put the site of reduction at about 3.7 Å from the electrode surface, which is a reasonable value for the adsorption mechanism. In such a case agar should decrease the rate of reduction instead of increasing it. Also the simultaneous passage of two electrons in the electron transfer mechanism is unlikely. Thus one electron is probably

involved in the rate-determining step, and $\alpha = 0.670$. The site of reduction is then 7.5 Å from the electrode surface. Chloride ion had virtually no effect on the activation energies, giving no clue as to the probable mechanism. The decrease in the free energy of activation from 24.0 kcal to 22.7 kcal in the presence of agar suggests that the adsorbed agar may favor the passage of electrons much in the same way as in the nickelous case. The fact that α_n in the agar solutions increased markedly with temperature suggests that the presence of agar might make one path more favorable at the expense of another. The behavior of this ion should be studied more thoroughly.

(3) The reduction of ferrous ion. Since α_n is greater than unity, two electrons must be involved in the rate-determining step; α is then 0.522, and the site of reduction is 5.8 Å from the electrode surface. This distance places the reducible ion right in the solution side of the electrical double layer, where the simultaneous passage of two electrons is more probable than at a larger distance. The influence of adsorbed agar far out into the solution is not known, but from the evidence of the nickelous and cobaltous cases it is probably more than 5.8 Å. Why agar would then have no influence on the ferrous reduction is puzzling. Perhaps there is no complexing between ferrous ion and agar. The activity coefficients of aqueous solutions of FeCl_2 are lower than those of CoCl_2 and NiCl_2 , indicating that there should be more complexing of ferrous ion by chloride ion than the other two. The differences in activation energies between the 0.1 N NaClO_4 and 0.1 N NaCl solutions for ferrous ion were smaller than the experimental error, intimating that any complexing effect of chloride does not change the mechanism. The heat and entropy of activation of the 25°C ferrous

species could be obtained if ferrous ion were studied in the temperature range of 0 to 30°C instead of from 25 to 50°C. The observed distortion should be studied more thoroughly by the more accurate method outlined above.

Conclusions.

It is concluded from the kinetic studies on the mechanism of electroreduction at the dropping mercury electrode that:

(1) The aquo nickelous ion is reduced through the electron-transfer mechanism with the rate-determining step the introduction of one electron to form the unipositive state which is then rapidly reduced to the metal. The site of reduction is 10 Å from the electrode surface. Chloride ion lowers the heat of activation by providing a pathway of lower energy for the passage of electrons to the nickelous ion. Agar produces the same effect as chloride ion.

(2) The aquo cobaltous ion is probably reduced by the electron transfer mechanism. The rate determining step is the introduction of the first electron to an ion 7.5 Å from the electrode surface. Chloride ion had no effect on the mechanism. The possibility exists that two mechanisms are in competition with each other. This needs further study.

(3) The aquo ferrous ion is reduced by the simultaneous introduction of two electrons to an ion at a site 5.8 Å from the electrode surface. A new ferrous species was observed to form above 40°C. Chloride and agar had no effect on the reduction of ferrous ion. The aquo ferrous ion should be studied more completely between 0 and 30°C.

Chapter 4

THE FORMATION OF UNIPOSITIVE NICKEL BY ELECTROLYSIS IN CONCENTRATED
SALT SOLUTIONS

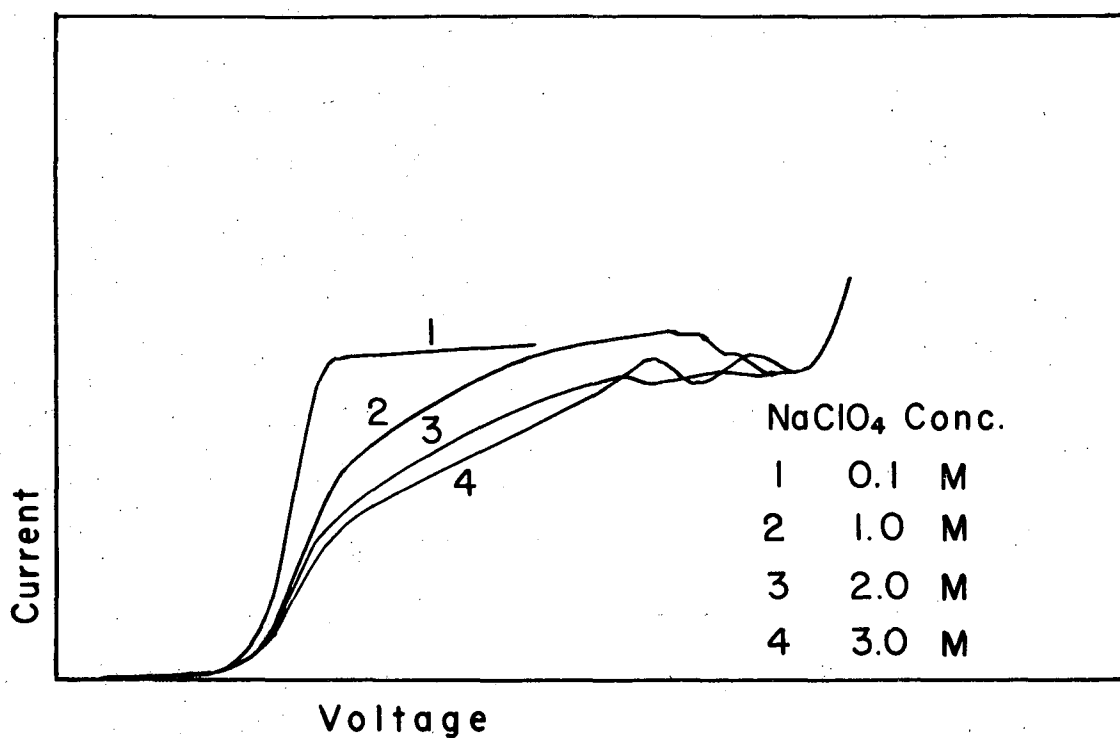
In the course of a study of the mechanism of the electroreduction of the first transition-group metal ions, it was found that nickelous ion shows a marked difference in behavior from the rest of this group in concentrated salt solutions. This chapter deals with the study of the reduction of Ni(II) in concentrated salt solutions and the evidence that Ni(I) is the primary reduction product under certain conditions. The experimental apparatus is the same as described in Chapter 3.

Current-voltage Curves of Nickelous Ion in Concentrated Solutions of Various Salts.

Current-voltage curves of Ni(II) in NaClO_4 solutions from 0.1 to 3.0 M are shown in Fig. 15. Curve 1 in Fig. 15 is a single continuous current-voltage curve corresponding to complete reduction to the metal. In curves 2, 3, and 4, the curves corresponding to the current-voltage curve observed in 0.1 M NaClO_4 split into two distinct portions. Apparently a limiting form of the C.V. curve is obtained as the concentration of NaClO_4 reaches 3.0 M. In curves 2, 3, and 4, a current corresponding to the diffusion current in curve 1 is not reached until some 0.5 volts from the start of the curve. In the light of data presented in Chapter 3 and subsequently in this chapter the curves in Fig. 15 can be interpreted as follows. In Chapter 3 it was shown that the rate-determining step in the electroreduction of nickelous ion is probably the introduction of one electron to form unipositive nickel. The rate constant for reducing the unipositive nickel must be very much larger than for reducing Ni(II) to Ni(I). In 3.0 M NaClO_4 , however,

the rate constant for the reduction of Ni(I) is much smaller than for the reduction of Ni(II) to Ni(I), and stepwise reduction of Ni(II) to the metal is observed. This results in an extended type of current-voltage curve. In this regard it is of interest to note that the height of the first portion of the current-voltage curve in 3.0 M NaClO₄ is slightly less than half that of the total wave when correction for change in drop time with increased potential has been made. This evidence indicates that the first portion of the total curve corresponds to the reduction of Ni(II) to Ni(I), and the second portion to the reduction of Ni(I) to the metal. The heights of both portions were found to vary linearly with concentration of Ni(II), as predicted by the Ilkovic equation. The height of the first portion of the current-voltage curve is referred to hereafter as i_1 .

Current-voltage curves of Ni(II) in NaCl solutions from 0.1 to 3.0 M containing 0.001 M HCl are shown in Fig. 16. Curve 1 in Fig. 16 is a current-voltage curve of Ni(II) in 0.1 M NaCl that corresponds to complete reduction to the metal. Curves 2, 3, and 4 indicate that the reduction of Ni(II) in concentrated NaCl solutions is similar to the reduction in concentrated NaClO₄. Much of the second portion of the curve is obscured by a rise in current resulting from the reduction of hydrogen ion, but it appears that the rate constant for the reduction of Ni(I) in concentrated NaCl solutions is even less than in concentrated NaClO₄. Apparently chloride ion is capable of stabilizing the Ni(I) to some extent. In curve 4 the Ni(I) is almost completely stabilized with respect to further reduction. It should be noted that the Ni(I), which is about 0.001 M, need only have a half-life greater than a few milliseconds to account for curve 4.



MU-10502

Fig. 15. Current-voltage curves of ca. 0.8 mmolar nickel in NaClO₄ solutions.

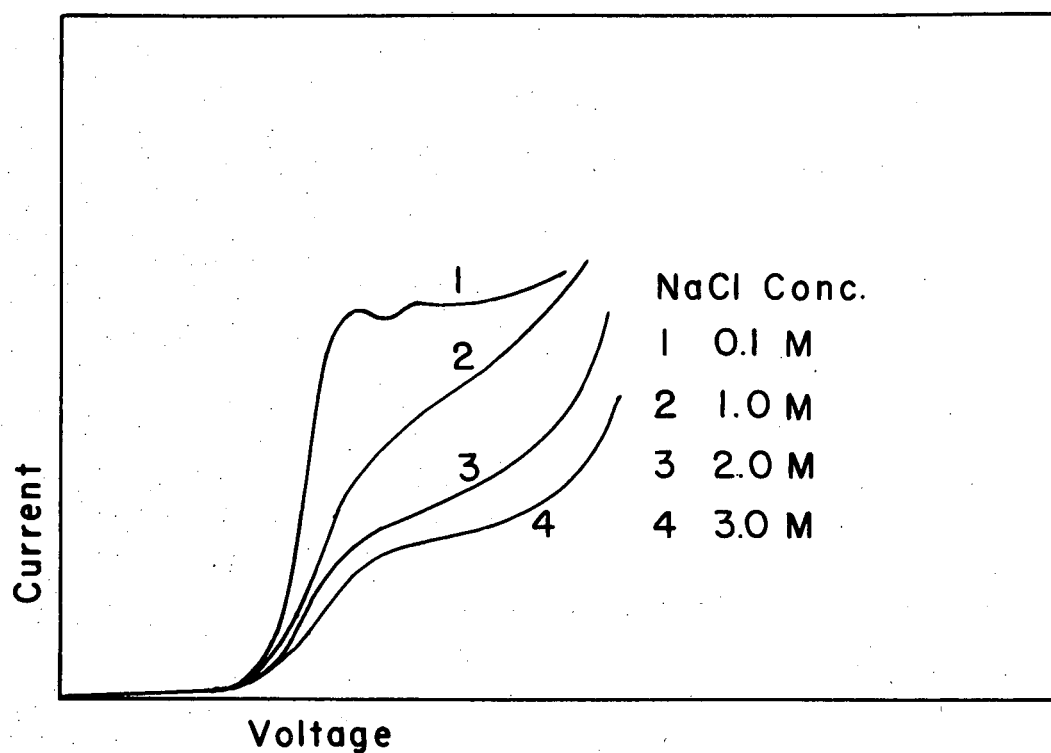
Current-voltage curves of Ni(II) have also been obtained over the concentration range 0.1 to 3.0 M in KCl, LiClO₄, and Ca(ClO₄)₂ solutions. In these cases the curves show the same general behavior as those presented in Figs. 1 and 2. In particular, the ratio of i_1 in the more concentrated salt solutions to the diffusion current in 0.1 M salt is almost constant at any given concentration of each of the salts. The effect of all of these salts is remarkably similar when compared at the same concentration level. This stepwise reduction of Ni(II) is also observed in 3 M NH₄Cl and 2 M NaAc.

Whatever the explanation may be it appears that the "stabilization" of Ni(I) is not a specific property of a given salt but is primarily dependent upon the magnitude of the salt concentration.

Comparison of Calculated and Observed Limiting Currents in NaClO₄ Solutions.

The measured diffusion coefficients of Ni(II) in 0.1 M NaClO₄ and 3.0 M NaClO₄ are 0.60×10^{-5} and 0.56×10^{-5} cm²/sec respectively.²⁶ From these values using the equation of Lingane and Loveridge⁵ the calculated diffusion current is 7.15 ± 0.3 microamperes in 0.1 M NaClO₄ assuming complete reduction to the metal. The observed value is 6.84 ± 0.2 . The calculated value in 3.0 M NaClO₄ is 6.90 ± 0.3 for reduction to the metal and 3.45 ± 0.15 for reduction to Ni(I). The observed i_1 in 3.0 M NaClO₄ is 2.94 ± 0.3 microamperes. This is in agreement with the assumption that Ni(I) is the primary product in the concentrated salt solution.

The above result does not rule out the possibility that two species of Ni(II), reducible at different potentials, are obtained in these concentrated salt solutions. It does seem very unlikely that this would



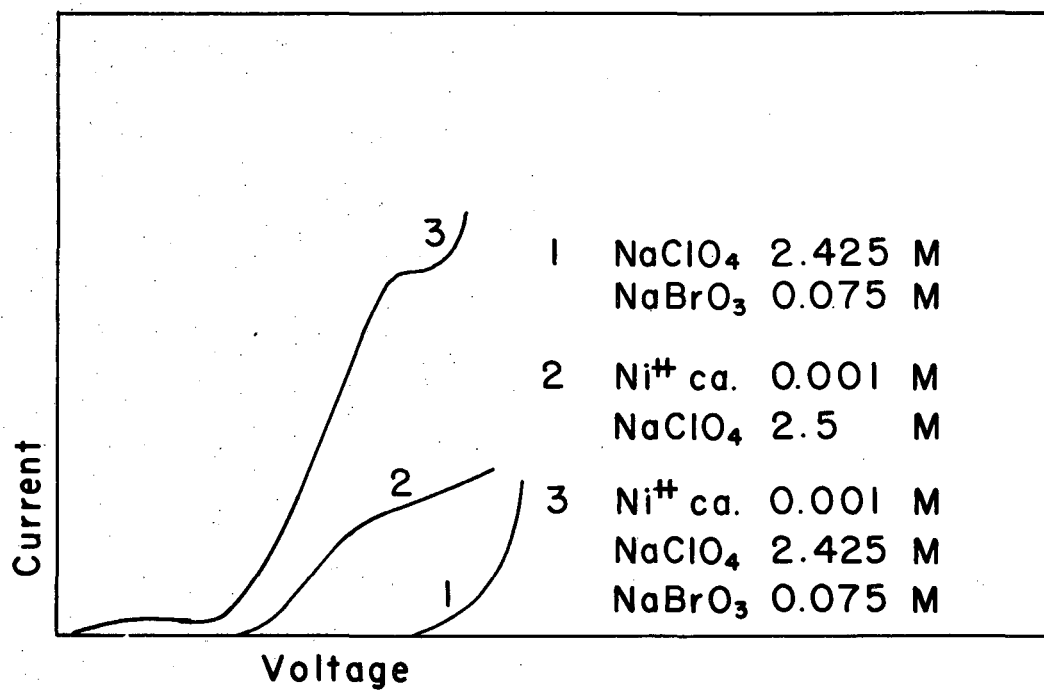
MU-10503

Fig. 16. Current-voltage curves of ca. 1 mmolar nickel in NaCl solutions, pH 3.

occur in such a similar fashion for the variety of salts studied.

Evidence for Ni(I) by Reaction with Bromate.

The current-voltage curves of Ni(II) in 0.1 M NaBrO₃ are the same as in 0.1 M NaClO₄. This shows that there is no direct catalysis of bromate reduction by Ni(II) nor any reaction between bromate and the Ni amalgam formed. However, in more concentrated NaClO₄ solutions with bromate present there is a reaction, as shown by the curves in Fig. 17. The greatly increased current observed in the presence of bromate in curve 3 of Fig. 17 combined with the fact that no such effect is found when Ni amalgam is produced in the dilute salt solutions seems to be good evidence that the reactive intermediate Ni(I) is formed in the more concentrated salt solution. If the bromate concentration is reduced below 0.01 M the rate of reaction with Ni(I) apparently becomes too slow for this effect to appear. The augmented diffusion current may be analyzed by equations developed by Koutecky³³ for diffusion currents produced by a combination of diffusion and reaction. It is assumed that the observed current is due to nickel only, and none to intermediate bromate reduction products. This assumption probably is not correct, but it sets an upper limit on the rate constant. With the total sodium ion concentration 2.5 M, and bromate and perchlorate as anions, an average bimolecular rate constant of 43 ± 10 liters mole⁻¹ sec⁻¹ was calculated. This theory also predicts that the total current should be linear with Ni(II) concentration at a given bromate concentration, and this was found to be so. It was also found that there is no apparent reaction of Ni(I) with bromate in concentrated NaCl solution. This may reflect the influence of chloride ion on the rate of reaction of bromate with Ni(I).



MU-10504

Fig. 17. Current-voltage curves of nickel-bromate systems.

Determination of the Amount of Nickel Metal Produced in Electrolysis.

Appropriate salt solutions containing 0.01 M Ni(II) were electrolyzed with the dropping mercury electrode for about two hours. The mercury was collected and analyzed for nickel content. The nickel was extracted with concentrated HCl overnight, with intermittent stirring. The solution was taken and analyzed for nickel by the polarographic method with 0.1 M KCl as the supporting electrolyte. The amount of Ni found was compared to that calculated from the observed average current at potentials corresponding to i_1 and the time of electrolysis. If metallic nickel is the reduction product 100% of the calculated amount of Ni should be recovered. If Ni(I) is the only product and no metallic nickel is formed by reaction at the mercury surface before actual collection of the drops, no Ni should be observed. It is probable that some metallic nickel is formed by disproportionation at the surface of the Hg as the drops fall and are collected. The present experimental techniques are subject to several percent error due to uncertainty in the quantity of electricity employed and in the efficiency of the Ni recovery method. The results are tabulated in Table 10.

Table 10

Percent Recovery of Nickel from Amalgams, Current Equivalence Basis	
<u>Salt</u>	<u>% Ni</u>
0.1 <u>M</u> NaClO ₄	96
3.0 <u>M</u> NaClO ₄	68
2.5 <u>M</u> NaClO ₄ and 0.5 <u>M</u> NaBrO ₃	5
0.1 <u>M</u> NaCl	96
3.0 <u>M</u> NaCl	89
2.9 <u>M</u> NaCl and 0.1 <u>M</u> NaBrO ₃	28

These data indicate quite clearly that unipositive nickel is the initial reduction product in concentrated solutions of supporting electrolytes.

Unipositive nickel in the presence of other reactants. No change was observed in the nickel wave in 2.0 M NaClO₄ when either permanganate or ceric ion was added to the solution in small concentration. These are reduced at the electrode, of course, and apparently were not present in large enough concentration about the electrode to produce a noticeable interaction. The nickel (I) might be reduced by a strong reducing agent like chromous ion. Chromous is the reduction product of chromic at potentials below the nickel reduction, and its oxidation by nickel (I) would lead to an increase in the total current observed. However, the observed total current was merely a summation of the chromic and nickel diffusion currents.

The disproportionation mechanism of nickel reduction. If the normal reduction of nickel in dilute solutions of supporting electrolytes involves the disproportionation of unipositive nickel, where the rate is so large that a limiting diffusion current of twice that from a one-electron reduction is obtained,³⁴ then in the intermediate salt concentrations the "diffusion current" should not be linear with concentration of nickel. The diffusion current of nickel in 1.0 M NaClO₄ was taken as the height of the first portion of the total wave, and was found to be linear with nickel concentration up to 0.01 M nickel. This result indicates that the rate of disproportionation must be slow compared to the rate of diffusion of Ni(I) away from the electrode surface.

Attempts at electrochemical identification. Nickel (II) in saturated NaCl was electrolyzed with a small mercury pool at 14°C, then some of the solution just above the pool was quickly pipetted into a ferric-

ortho-phenanthroline solution and the transmittance was observed with a colorimeter. The Ni(I), if present, should reduce the ferric-ortho-phenanthroline complex to the highly colored ferrous-ortho-phenanthroline complex. The transmittance was the same as the solution gave before electrolysis. This indicates either that the rate of reaction of the ferric complex with Ni(I) must be slow compared to the lifetime of Ni(I), or that the lifetime of Ni(I) is shorter than one to two minutes, which is the period of transfer.

In another experiment, the above solution was electrolyzed for a short time with a small mercury pool, and an attempt was made to find an oxidizable species just above the surface of the pool with the dropping mercury electrode. There was none detectable above the potential of the dissolution of mercury.

A dropping mercury electrode with a drop time of six seconds was used with a switching device to change from a potentiometer to the polarograph. The drop was allowed to form for two seconds, with an applied potential great enough to reduce nickel, when the arrangement was switched to the polarograph at a potential just below the nickel wave. With a concentrated NaCl solution, a small oxidation current was observed, but the same result was found in the dilute solution.

The temperature dependence of the limiting current. The temperature dependence of i_1 in 2 M NaClO₄ was determined and was found to be linear, but greater than for 0.1 M NaClO₄. This indicates that there is an added factor controlling the diffusion current in the more concentrated solution. The factor could be one of kinetics or equilibrium between two different species.

Nickel complex ions. When the nickel ammonia complex was reduced in a solution consisting of 0.5 M NH_4OH and 0.1 M NH_4Cl , the diffusion current when the solution was also 3.0 molar in NaCl was 85% that found when 0.1 M NaCl was present. The diffusion current due to the complex $\text{Ni}(\text{OAc})_2$ in 2.0 M NaOAc is about half that obtained in 0.1 M NaOAc , where two-thirds of the nickel is uncomplexed. In addition, the diffusion current plateau is much flatter than in the other cases. The acetate complex probably has at least four waters still bound to the nickel ion, while in the ammonia complex all the water is displaced. The evidence suggests that the stabilization of $\text{Ni}(\text{I})$ is related in some fashion to the type of complexing.

Discussion. The points that clearly seem to identify unipositive nickel are

- (1) The nickel wave is divided into two portions of approximately the same size in the presence of a high concentration of supporting electrolyte;
- (2) A definite interaction between bromate ion and a reactive nickel reduction product has been observed, but only in the presence of a large concentration of supporting electrolyte;
- (3) Less nickel is recovered from nickel amalgams formed out of solutions containing a large excess of supporting electrolyte.

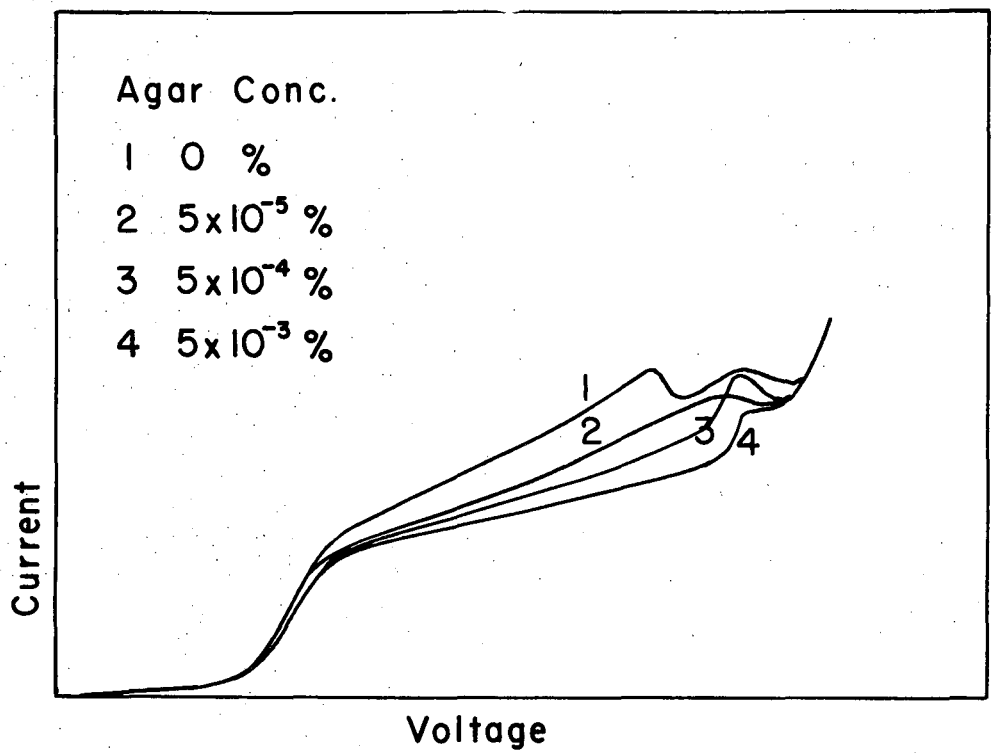
When bromate is added much less is obtained.

For $\text{Ni}(\text{I})$ to exist in a concentration less than 0.1% that of $\text{Ni}(\text{II})$ in the presence of Ni, the potential for the reaction $\text{Ni}(\text{I}) = \text{Ni}(\text{II}) + e^-$ must be greater than about 0.46 volt vs. NHE. From the observed electrode reduction potential of $\text{Ni}(\text{II})$ the reversible potential for the reaction $\text{Ni}(\text{I}) = \text{Ni}(\text{II}) + e^-$ could be no more than 0.75 volt vs. the NHE.

Thus the potential of the couple $\text{Ni} = \text{Ni}^+ + e^-$ must be between the limits of ± 0.04 volt and -0.25 volt vs. NHE. The high salt concentration must slow the rate of the electroreduction of Ni(I). This stabilization could result from a change in the Ni(I) species. The change could be in the number of complexed groups or in the complexing of the salt.

The only Ni(I) compound known is the complex cyanide. There is some controversy as to whether the composition of the compound is $\text{K}_2\text{Ni}(\text{CN})_3$ or $\text{K}_3\text{Ni}(\text{CN})_4$. In the former complex Ni(I) would be tricoordinated, while in the latter, tetracoordinated. Ni(I) would have the same electronic configuration as Cu(II), where tetracoordination is the most stable. The increased salt concentration might promote the formation of a tri- or tetracoordinated species from the reduction product of Ni(II). The spectrum of Ni(II) in 3.0 M NaClO_4 was determined and was found to be identical within experimental error with the spectrum obtained with Ni(II) in 0.1 M NaClO_4 . This evidence indicates that hexacoordinated Ni(II) is also formed in 3.0 M NaClO_4 . Since $E_{1/2}$ for the reduction of Ni(II) is virtually unchanged, it is doubtful that any change in the Ni(II) species has taken place. Any change in the Ni(I) species by the high salt concentration has to take place after the Ni(I) has been formed at the electrode surface.

Another explanation for the formation of Ni(I) might lie in the fact that in such concentrated solutions it may be possible to limit the access of Ni(I) to the negatively charged electrode surface because of the high positive ion concentration that would prevail. This factor would only slow the rate of the reduction of Ni(I) at the electrode.



MU-10505

Fig. 18. The effect of agar on the current-voltage curves of ca. 0.8 mmolar nickel in 3.0 M NaClO_4 .

Alteration of the surface of the mercury drop by the adsorption of agar also slows the introduction of the second electron, as shown by Fig. 18. Whether this stabilization is the result of blocking the surface or a complexing effect cannot be determined.

The most logical explanation for the stabilization of Ni(I) is a change in the Ni(I) species. To see if the activity of water was involved, the diffusion current of Ni(II) was measured as a function of methyl or ethyl alcohol concentration, up to 50% alcohol. The diffusion current was lowered, but the same effect was observed by Matsuyama for many ions.³⁵ The single continuous current-voltage curves had the same form as that observed in 0.1 M NaClO_4 , showing no evidence for an intermediate product.

Conclusion. Unipositive nickel has been identified as a reduction product of nickel (II) at the dropping mercury electrode in the presence of a high concentration of supporting electrolyte. The stabilization of Ni(I) in these solutions could arise from either a change in the Ni(I) species or a blocking of the electrode surface by the high positive ion concentration that would be present.

ACKNOWLEDGMENT

The author wishes to express his sincere thanks to Professor Edwin F. Orlemann for his patient and careful guidance through all phases of this work; to the University of California and the University of California Radiation Laboratory for financial assistance; and to that large number of people who have been of constant inspiration.

This work was done under the auspices of the U.S. Atomic Energy Commission.

REFERENCES

1. Glasstone, S., Laidler, K. J., and Eyring, H., "The Theory of Rate Processes," McGraw-Hill Book Co., Inc., New York (1941), p. 575.
2. Kolthoff, I. M., and Lingane, J. J., "Polarography," Interscience Publishers, New York (1952), p. 297.
3. Ilkovic, D., Collection Czechoslov. Chem. Commun. 6, 498 (1934).
4. MacGillivray, D., and Rideal, E. K., Rec. trav. chim. 56, 1013 (1937).
5. Lingane, J. J., and Loveridge, B. A., J. Am. Chem. Soc. 72, 438 (1950).
6. Koutecky, J., Czechosl. Journ. Phys. 2, 50 (1953).
7. Koutecky, J., Collection Czechoslov. Chem. Commun. 18, 597 (1953).
8. Grahame, D. C., Chem. Reviews 41, 441, (1947).
9. Volmer, M., Physik. Z. der Sowjetunion 4, 346 (1933).
10. Orlemann, E. F., and Kolthoff, I. M., J. Am. Chem. Soc. 64, 1044 (1942).
11. Lewis, M., Ph.D. Thesis, University of California (1950).
12. Koutecky, J., Chem. Listy 47, 323 (1953).
13. Delahay, P., and Strassner, J. E., J. Am. Chem. Soc. 73, 5219 (1951).
14. Evans, M. G., and Hush, N. S., J. chim. phys. 49, C159 (1952).
15. Kivalo, P., Oldham, K. B., and Laitinen, H. A., J. Am. Chem. Soc. 75, 4148 (1953).
16. Gurney, R. W., Proc. Royal Soc. A134, 137 (1931).
17. Bates, L. F., and Fletcher, W. P., Proc. Phys. Soc. 51, 778 (1939).
18. Tamman, G., and Arntz, F., Z. anorg. allgem. Chem. 192, 45 (1930).
19. Silverman, J., and Dodson, R. W., J. Phys. Chem. 56, 846 (1952).
20. Goldberg, I., and Jura, G., Unpublished Experiments.
21. Taube, H., Chem. Reviews 50, 69 (1952).
22. Powell, R., and Latimer, W. M., J. Chem. Phys. 19, 1139 (1951).
23. Williams, R. J. P., J. Phys. Chem. 58, 121 (1954).

REFERENCES

(-2-)

24. Quill, L. L., Ed., "The Chemistry and Metallurgy of Miscellaneous Materials," McGraw-Hill Book Co., Inc., New York (1950), p. 165.
25. Kolthoff, I. M., and Stenger, V. A., "Volumetric Analysis," 2nd edition, Vol. II, p. 284, Interscience Publishers, Inc., New York (1947).
26. Sanborn, R. H., and Orlemann, E. F., J. Am. Chem. Soc. 77, 3726 (1955).
27. Oholm, L. W., Finska Kemistam fundets Medd. 45, 133 (1936); C.A. 31, 2904.
28. Kolthoff, I. M., and Lingane, J. J., "Polarography," Interscience Publishers, New York (1952), p. 520.
29. Leussing, D. L., and Kolthoff, I. M., J. Am. Chem. Soc. 75, 2476 (1953).
30. Gayer, K. H., and Woontner, L., J. Am. Chem. Soc. 74, 1436 (1952).
31. Wingfield, B., and Acree, S. F., J. Research Nat'l Bur. Standards 19, 163 (1937).
32. Kolthoff, I. M., and Lingane, J. J., "Polarography," Interscience Publishers, New York (1952), p. 203.
33. Koutecky, J., Collection Czechoslov. Chem. Commun. 18, 311 (1953).
34. Orlemann, E. F., and Kern, D. M. H., J. Am. Chem. Soc. 75, 3058 (1953).
35. Kolthoff, I. M., and Lingane, J. J., "Polarography," Interscience Publishers, New York (1952), p. 98.